Pseudo-nitzschia Bloom Dynamics in the Gulf of Maine: 2012–2016

Suzanna Clark^{a*}, Katherine A. Hubbard^{a,b}, Donald M. Anderson^a, Dennis J. McGillicuddy, Jr.^a, David K. Ralston^a, David W. Townsend^c

^aWoods Hole Oceanographic Institution, 86 Water St. MS 21 Woods Hole, MA USA 02543

^bFlorida Fish and Wildlife Conservation Commission-Fish and Wildlife Research Institute, 100 8th Ave SE, St. Petersburg, FL USA 33701

^cUniversity of Maine, Orono, ME 04469

E-mail addresses: sclark@whoi.edu (Suzanna Clark), Katherine.Hubbard@myfwc.com (Katherine Hubbard), danderson@whoi.edu (Donald Anderson), mcgillic@whoi.edu (Dennis J. McGillicuddy, Jr.), dralston@whoi.edu (David Ralston), davidt@maine.edu (David Townsend)

^{*} Corresponding Author

Abstract

The toxic diatom genus *Pseudo-nitzschia* is a growing presence in the Gulf of Maine (GOM), where regionally unprecedented levels of domoic acid (DA) in 2016 led to the first Amnesic Shellfish Poisoning closures in the region. However, factors driving GOM Pseudo-nitzschia dynamics, DA concentrations, and the 2016 event are unclear. Water samples were collected at the surface and at depth in offshore transects in summer 2012, 2014, and 2015, and fall 2016, and a weekly time series of surface water samples was collected in 2013. Temperature and salinity data were obtained from NERACOOS buoys and measurements during sample collection. Samples were processed for particulate DA (pDA), dissolved nutrients (nitrate, ammonium, silicic acid, and phosphate), and cellular abundance. Species composition was estimated via Automated Ribosomal Intergenic Spacer Analysis (ARISA), a semi-quantitative DNA finger-printing tool. Pseudo-nitzschia biogeography was consistent in the years 2012, 2014, and 2015, with greater Pseudo-nitzschia cell abundance and P. plurisecta dominance in low-salinity inshore samples, and lower Pseudo-nitzschia cell abundance and P. delicatissima and P. seriata dominance in highsalinity offshore samples. During the 2016 event, pDA concentrations were an order of magnitude higher than in previous years, and inshore-offshore contrasts in biogeography were weak, with P. australis present in every sample. Patterns in temporal and spatial variability confirm that pDA increases with the abundance and the cellular DA of *Pseudo-nitzschia* species, but was not correlated with any one environmental factor. The greater pDA in 2016 was caused by P. australis – the observation of which is unprecedented in the region – and may have been exacerbated by low residual silicic acid. The novel presence of *P. australis* may be due to local growth conditions, the introduction of a population with an anomalous water mass, or both factors. A definitive cause of the 2016 bloom remains unknown, and continued DA monitoring in the GOM is warranted.

Keywords

Pseudo-nitzschia australis, Pseudo-nitzschia plurisecta, Domoic Acid, ARISA, Gulf of Maine, silicic acid

1 Introduction

Domoic acid (DA) first came to international attention in 1987, when hundreds of people were poisoned and three people died after eating contaminated shellfish harvested on Prince Edward Island, Canada. The diatom Nitzschia pungens was identified as the culprit (Bates et al., 1989). Since then, Nitzschia pungens has been re-classified as Pseudo-nitzschia multiseries, 52 more Pseudo-nitzschia species have been identified, and 26 species have been shown to produce DA (Bates et al., 2018). Pseudo-nitzschia are typically lightly-silicified, cosmopolitan diatoms (Hasle, 2002) that have been found along the coastlines of every continent in the world (Trainer et al., 2012) and can tolerate a broad range of environmental conditions. Some species, such as P. seriata, can grow in temperatures from 4°C (Hansen et al., 2011) to 15°C (Fehling et al., 2004), and others, such as P. multiseries, can grow in salinities from 20 to 40 (Doucette et al., 2008; Thessen and Stoecker, 2008).

Toxic *Pseudo-nitzschia* blooms are traditionally associated with upwelling regions, but the genus has also been observed in oligotrophic gyres (Guannel et al., 2015), bays (Thorel et al., 2017) and shelf seas (Bresnan et al., 2015). Regime shifts in *Pseudo-nitzschia* absolute and relative abundance have been connected to changes in nutrient ratios (Lundholm et al., 2010; Parsons et al., 2002), remote physical forcing (Sekula-Wood et al., 2011), and temperature (Lundholm et al., 2010). In recent years, globally and regionally record-breaking blooms (in terms of DA concentrations and the extent of shellfishery closures) have occurred (McCabe et al., 2016; Bates et al., 2018)). In the Gulf of Maine (GOM), nine unique species of *Pseudo-nitzschia* had been identified as of 2014 (Fernandes et al., 2014) and in 2016 an unprecedented bloom of *P. australis* led to the first regional observations of shellfish DA concentrations exceeding the regulatory limit of 20 μ g DA g⁻¹ shellfish tissue (Bates et al., 2018). Beginning in mid-September, DA in shellfish tissue in the Bay of Fundy exceeded 18 μ g DA g⁻¹ shellfish tissue and it remained elevated through the end of the month (Canadian Food Inspection Agency, 2016). Along the coast of Maine, clam and mussel harvesting was suspended sequentially from the northeast to the southwest, beginning with Cobscook Bay at the Canadian border on September 27, continuing to Mount

Desert Island by September 30, and eventually growing to include Penobscot Bay by the first week of October (refer to Figure 1 for location references) (Rappaport, 2016).

Threats to economic and human health, along with *Pseudo-nitzschia*'s apparent growing presence, have motivated studies about the factors – biogeochemical, ecological, and physical – controlling *Pseudo-nitzschia* blooms. Studies on *Pseudo-nitzschia* growth have argued that, because *Pseudo-nitzschia* are often lightly silicified relative to other diatoms, they are most competitive in waters with low silicate- (or silicic acid)-to-nitrate ratios (Marchetti et al., 2004; Parsons et al., 2002), in that they thrive when there is sufficient nitrogen to support protein synthesis, but too little silicic acid for other diatom species. Other studies have connected species-specific growth rates to specific temperatures (Santiago-Morales and García-Mendoza, 2011) or salinities (Doucette et al., 2008). *Pseudo-nitzschia* have been linked to hydrodynamic features, such as the Juan de Fuca Eddy, which acts as an incubation site for *Pseudo-nitzschia* blooms (Trainer et al., 2002). In the Santa Barbara Channel, convergent eddies were found to aggregate pre-existing, low density blooms until their densities increased from 5*10⁵ to more than 2*10⁶ cells L⁻¹ (Anderson et al., 2006). Bloom development and transport has also been connected to wind direction and upwelling conditions in Washington (MacFadyen et al., 2005), California (Schnetzer et al., 2013), Portugal (Palma et al., 2010), and Ireland (Cusack et al., 2015).

Cell growth is not the only factor controlling DA concentrations in a *Pseudo-nitzschia* bloom: inter- and intraspecific variation in DA production depend on environmental conditions. DA production has been connected to iron limitation, low silicic acid concentrations, increased pH, increased salinity, the presence of predators, light availability, and sometimes even multiple, compounding factors (as reviewed in Bates et al., 2018; Trainer et al., 2012). In addition, laboratory studies do not always translate to the field, where multiple factors change simultaneously and pathways towards DA production are complex. Several field studies have concluded that *Pseudo-nitzschia* DA production in the field cannot be attributed to one single environmental parameter (Smith et al., 2017; Trainer et al., 2009).

Pseudo-nitzschia in the GOM have not been extensively studied, but their growing presence and particularly the DA event in 2016 motivate the need to understand the dynamics of the genus in

this region. DA poses a threat both to the economy and to human health. However, because of the disconnect between laboratory results and field observations, the varied theories about DA production, and the range of possible *Pseudo-nitzschia* growth conditions in the field, it is challenging to draw conclusions on Pseudo-nitzschia or DA dynamics based entirely on information from the literature.

This paper explores the biogeography of *Pseudo-nitzschia* species in the GOM from 2012–2016. Environmental factors controlling species composition and toxic Pseudo-nitzschia blooms are explored through descriptive and statistical analysis of genetic species, nutrient, and hydrodynamic data. The effects of environmental factors and species composition on DA are analyzed. Special attention is given to explaining the 2016 bloom and exploring factors that led to the highest pDA concentrations ever recorded in the GOM.

Methods 2 67

56

57

58

59

60

61

62

63

64

65

66

69

71

75

76

79

80

81

82

2.1 Study Site 68

The GOM is a coastal sea on the North American East Coast that stretches from Cape Cod, 70 Massachusetts at 42°N to the Bay of Fundy at 44.5°N (Figure 1A). Mean sea surface temperature ranges from ~6°C in February to ~22.5°C in August, and salinity ranges from 29 to 33.5 (Li and He, 72 2014). The five largest rivers that feed into the GOM are, in order of decreasing volume flux, the St. John River, Penobscot River, Kennebec River, Androscoggin River, and Merrimack River (Li et 73 74 al., 2014). Because of resonance of the M2 tide, the GOM is home to some of the largest tidal amplitudes in the world: tidal amplitudes at the northern end of the Bay of Fundy can reach 6 m (Lynch and Naimie, 1993). This tidal energy can fully mix the water column in the Northeastern 77 Gulf, Bay of Fundy, Eastern Maine Coastal Current, and on the crest of Georges Bank, providing 78 an important mechanism to transport nutrients to the surface (Townsend et al., 2014).

The GOM is comprised of three deep basins, Jordan Basin, Georges Basin, and Wilkinson Basin, which are each deeper than 200 m. Exchange between the GOM and the Atlantic shelf sea is restricted by the shallow (< 100 m) Browns Bank and Georges Bank. Inflows occur via slope water from the North Atlantic entering through the Northeast Channel or Scotian Shelf Water flowing

- around the tip of Nova Scotia towards the Bay of Fundy, and outflows occur through both the South Channel and the Northeast Channel (Xue et al., 2000). The general circulation in the GOM
- is cyclonic, with anti-cyclonic flow around Georges Bank.
- 86 Alongshore transport in the GOM is driven by the coastal-trapped river plume and the Gulf of
- 87 Maine Coastal Current (GMCC) (Bisagni et al., 1996; Pettigrew et al., 2005). The pressure-
- 88 gradient-driven GMCC connects the eastern GOM to the western GOM, and has been shown to
- be important to Alexandrium catenella bloom dynamics (Keafer et al., 2005; Li et al., 2009), but
- 90 the strength of the connection varies interannually (Pettigrew et al., 2005). As shown by
- 91 McGillicuddy et al. (2011), several hydrodynamic processes, including upwelling winds,
- 92 stratification, and alongshore transport, influence HAB dynamics in the GOM; anomalies in one
- process, in addition to biological factors, could create conditions for an extremely large bloom,
- 94 or none at all.

95 2.2 Biological Data – Ship Surveys

- Shipboard surveys were conducted on the R/V Tioga on August $4^{th} 5^{th}$ 2012, July $25^{th} 27^{th}$
- 97 2014, and August 2nd 5th 2015, and on the *R/V Gulf Challenger* on October 5th 7th 2016. Sample
- 98 stations were arranged in offshore transects centered on Mount Desert Island, Maine, and
- 99 extended up to 60 km offshore (Figure 1B). The number and locations of sample stations varied
- depending on weather and in response to *Pseudo-nitzschia* bloom locations: 25 stations were
- sampled in 2012, 36 in 2014, 40 in 2015, and 21 in 2016. At each station, discrete water samples
- were collected with Niskin bottles at 1, 10, 20, 30, 40 and 50+ m (site depending). Casts with a
- 103 CTD Sea-Bird 9 recorded temperature (°C), salinity, conductivity (siemens m⁻¹), transmissivity (1
- 104 m⁻¹), turbidity (NTU), dissolved oxygen (ml L⁻¹), and pressure (dbar).

105 2.2.1 Pseudo-nitzschia Data

- 106 Cell Counts. For cruise samples, 125 mL whole seawater samples from 1, 10, and 20 m were
- preserved with Lugol's fixative. A 3-mL aliquot was added to a 5-mL Nunc Lab-Tek 2-chamber
- 108 counting chamber (ThermoFisher) and Pseudo-nitzschia cells were enumerated with a Zeiss
- 109 Axiovert inverted light microscope at 200–400x magnification and categorized into two size

categories, small (<3 μ m in width) and large (>3 μ m in width), and two orientations, chain or single-celled. In 2016, an intermediate size category (~3 μ m in width) was added. The limit of detection (LOD) for cell counts by light microscopy was 333 cells L⁻¹. Absolute cell abundance was recorded as the total of all sizes and cell orientations.

Relative Species Abundance. Water samples were also analyzed for species composition via Automated Ribosomal Intergenic Spacer Analysis (ARISA) (Hubbard et al., 2014). After filtration of 125 mL of seawater onto 0.45 μ m pore size nitrocellulose filters (Millipore), filters were frozen shipboard with liquid nitrogen and stored at -80°C until extraction. DNA was extracted with a DNeasy Plant Mini Kit (Qiagen Inc.), amplified via polymerase chain reaction (PCR) with the Pseudo-nitzschia-specific ITS1 primer set PnALL F/R, and purified using MultiScreen PCR 96 filter plates (Millipore) as described in Hubbard et al., 2014. For ARISA, PCR products were standardized and 1 ng DNA was analyzed on an ABI 3730 XL. Electropherograms were analyzed using DAx software (Van Mierlo Software Consultancy, Eindhoven, Netherlands) to characterize amplicon sizes (for species association) and relative peak heights (for quantitative assessments) according to Hubbard et al., (2014). Amplicon sizes characterized by ARISA were identified by comparing results with the GenBank nucleotide (nr/nt) database and regional studies (summarized in and including Fernandes et al., (2014)). For the 2016 event, P. australis was identified using ITS1 sequencing (targeting the ARISA amplicon) of DNA from live chains (placed in 5 μ L DNA-free water and subjected to three freeze-thaw cycles) and extracts used for ARISA (see Smith et al. (2017)). P. australis identification was confirmed with scanning electron microscopy conducted on Lugol's preserved material (Bates et al., 2018).

2.2.2 Particulate Domoic Acid

110

111

112

113

114

115

116

117

118

119

120

121

122

123

124

125

126

127

128

129

130

131

132

133

134

135

136

137

For pDA analysis, 125–250 mL of seawater were filtered through a 0.45 μ m pore size nitrocellulose filter and frozen at -20°C until analysis. Prior to analysis, extracts were filtered through 0.22 μ m PVDF syringe filters. Extracts were analyzed using an Acquity UPLC system coupled to a Quattro MicroTM API triple quadrupole mass spectrometer operated in positive ionization mode (ESI+) according to a method adapted from Wang et al., (2007). Separations were performed on an Acquity UPLC BEH C18 1.7 μ m column (2.1 x 50 mm). Mobile phase

consisted of Nanopure water (A) and acetonitrile (B) in a binary system with 0.1% formic acid as an additive. The detection of domoic acid was achieved by multiple reaction monitoring (MRM) using optimized instrument parameters. MRM transitions from the protonated DA ion were monitored for the following transitions: m/z 312 > 248, and m/z 312 > 266 and m/z 312 > 193. The transition m/z 312 > 266 was used for quantitation. A certified reference solution of domoic acid purchased from the National Research Council, Halifax, Canada was used to generate a 9-point standard curve from 0.78-200 ng DA mL⁻¹. The limit of detection was defined as the level yielding a signal to noise ratio of 3. The limit of quantitation was defined as the lowest concentration on the standard curve (0.78 ng DA mL⁻¹) or the concentration that yielded a signal to noise ratio of 10 if that was greater than 0.78 ng DA mL⁻¹.

2.3 Biological Data – Mt. Desert Island Time Series

From 2013 to 2016, weekly water samples were collected from Mt. Desert Island Biological Laboratory (MDIBL) and Bar Harbor on Mt. Desert Island, Maine as part of the Maine Department of Marine Resources' volunteer phytoplankton monitoring program. Ten-liter water samples were concentrated to 15 mL using a 15 μ m sieve, which may not have captured all (especially smaller) *Pseudo-nitzschia* cells. For cell counts via light microscopy, a 1 mL sample was added to a gridded Sedgewick Rafter slide, and cells L⁻¹ were enumerated either by counting all cells or by estimating based on the grid number at which 500 cells were enumerated; cells were categorized as either "large" (>3 μ m in width) or "small" (<3 μ m in width). Species composition at Bar Harbor in 2013 was evaluated by ARISA (Section 2.2.1) and pDA was measured from whole seawater by LC-MS/MS (Section 2.2.2). Water temperature, salinity, and dissolved oxygen were measured with a handheld YSI (YSI Instruments, Yellow Springs, OH), and dissolved nutrient concentrations were measured from whole seawater samples according to the methods in Section 2.4.

2.4 Physicochemical Data

Nutrients. Ship survey water samples from 1, 10, and 20 m and Mt. Desert Island surface samples were analyzed for nitrate + nitrite (NO_x^-), ammonium (NH_4^+) silicic acid ($Si(OH)_4$), and phosphate (PO_4^{3-}). Samples were filtered through a 0.22 μ m acetate luer-lock syringe filter and frozen at -20°C until analysis. Dissolved NO_x^- , phosphate, and silicic acid concentrations were measured

with a QuickChem 8500 Flow Injection Analysis system, and dissolved ammonium concentrations
 were measured on a TD-700 fluorometer.

Oceanographic, Atmospheric, and Riverine Measurements. Buoys from the Northeastern Regional Association of Coastal Ocean Observing Systems (NERACOOS) have recorded temperature, salinity, conductivity, potential temperature, air temperature, air pressure, and wind speed at hourly intervals since 2001 (Morrison, 2019) (Figure 1B). Instruments were positioned at 1, 20, and 50+ m below the surface (site-depending), allowing for characterization of the vertical structure of the water column at high temporal resolution. Salinity and temperature data from buoys N, M, and I from 2001–2016 were used to characterize water mass characteristics and climatology. Wind speed and direction from station I were used to calculate the upwelling index from 2001 to 2016.

An upwelling index (UI) was calculated according to Schwing et al. (1996): $UI = \frac{\tau_x}{\rho f}$, where τ_x is the alongshore component of the wind stress as defined by Large and Pond (1981), ρ is the surface water density in kg m⁻³, and f is the Coriolis parameter. According to this convention, a positive UI indicates upwelling, while a negative UI indicates downwelling. Cumulative UI (CUI) was calculated by integrating UI over time from April through December in each year from 2001 to 2016.

The U.S. Geological Survey (USGS, 2013) and Canadian Water Office (Canada, 2018) report daily mean river discharge (m³ s⁻¹) for the St. John, Penobscot, Kennebec, Androscoggin, and Merrimack rivers. Cumulative river discharge was calculated in 2012–2016 by integrating daily discharge in m³ s⁻¹ over time to calculate m³.

Data used for this study are summarized in Table 1.

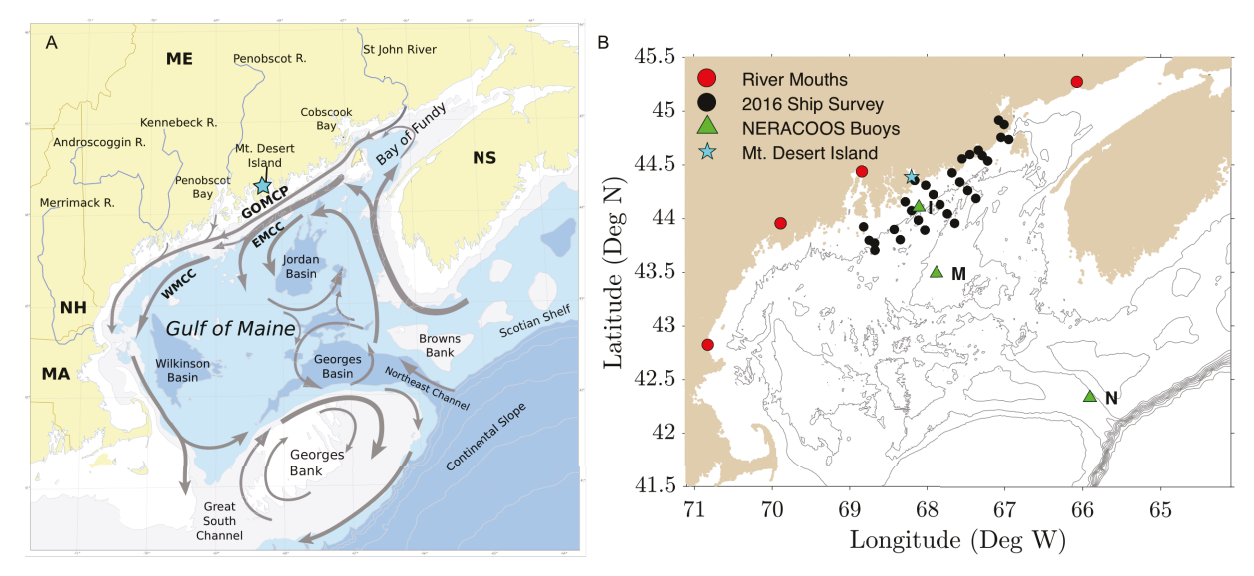


Figure 1 - (A) Climatological circulation of the GOM as described in Pettigrew et al., (2005) and adapted in Anderson et al., (2005) (Used with permission). (B) Locations of hydrographic instruments and the 2016 Pseudo-nitzschia ship survey in the GOM. "Mt Desert Island" is shown, where both MDIBL and Bar Harbor are located.

2.5 Descriptive and Statistical Analyses

Cell concentrations and species relative abundance were plotted at their sample locations to explore spatial variability. Each analysis described below was conducted on absolute cell abundance (cells L⁻¹), relative species abundance, chlorophyll, pDA, temperature, salinity, and dissolved nutrient concentrations. Relative nutrient concentrations were also analyzed including the silicic acid-to-total nitrogen ratio (Si(OH)₄:(NO_x⁻+NH₄⁺) or simply Si:N), silicic acid-to-phosphorous ratio (Si(OH)₄:PO₄³⁻ or Si:P), total nitrogen-to-phosphorous ratio ((NO_x⁻+NH₄⁺):PO₄³⁻ or simply N:P), and residual silicic acid ($Si^* = [Si(OH)_4] - [NO_x^-]$). Each year was analyzed individually, with all depths combined, except where indicated otherwise. For all statistical tests, correlations with a p-value < 0.05 were considered significant.

ARISA data were used in conjunction with pDA concentrations to estimate cellular DA (DA cell-1 or cDA), which varies widely among *Pseudo-nitzschia* species and is thus challenging to estimate from field data. Therefore, samples dominated by one species (relative abundance >85%) were selected, with exceptions made for samples as low as 70% relative abundance of the dominant species, as long as the other species were not associated with pDA in the dataset. Such allowances increased the number of samples to improve statistical robustness. If a sample had >85% relative abundance from the dominant species, but *P. australis* was also detected by ARISA,

then that sample was discarded because P. australis is known to produce pDA. PDA (μ g L⁻¹) was divided by the total cell concentration (cells L⁻¹) to find an estimate of cDA (pg cell⁻¹). The cDA calculation accounted for the relative abundance of the dominant species by dividing by its fraction of the sample:

213
$$\frac{DA}{cell} = \frac{pDA (Water Volume)^{-1}}{(relative abundance) * (cells (Water Volume)^{-1})}$$

Correcting by the relative abundance makes the assumption that DNA prevalence is proportional to cell counts, which is not necessarily correct. However, the calculation was also performed without adjusting for relative abundance, and the results varied little. The calculation was also performed with a lower minimum cutoff for relative abundance of the dominant species of 60%, and the main results did not change (refer to supplementary material).

Several statistical analyses were employed to quantify the relationships observed in the descriptive analysis. Linear least squares regression was used to explore correlations between species relative abundance, cell abundance, pDA and environmental parameters. Each species was tested against the environmental factors listed at the beginning of this section. Regression analysis was run for the cruise data and time series data, with each year individually, with all years combined, with all samples, and with only samples where pDA > LOQ.

Principal Component Analysis (PCA) was used to quantify variability in environmental factors and species relative abundance in the cruise data. Canonical Correspondence Analysis (CCA) was used to quantify correlations between environmental factors and community species composition in the cruise data. PCA and CCA were performed both on each year individually and on all years combined.

Lastly, the Wilcoxon signed rank test was used to test whether the measured environmental factors were statistically significantly different between years. This test was chosen because it does not assume normal sample distribution. Cruise data from 2016 were compared with other cruise data (2012, 2014, and 2015). Samples with pDA > LOQ were used, as the goal was to

234 determine the effect of different environmental factors on DA concentrations when toxic species 235 were already present. Results 236 Biogeography prior to 2016 237 238 3.1.1 Temporal Variability 239 Pseudo-nitzschia dynamics in the GOM exhibited interannual and seasonal variability in bloom 240 timing, cell abundance, and relative species abundance (Figure 2 and Figure 3). Notable patterns 241 are summarized below. 242 Interannual Variability. Maximum cell abundance was 75,000 cells L⁻¹ in 2012, 190,000 cells L⁻¹ in 2013, 65,000 cells L⁻¹ in 2014, and 180,000 cells L⁻¹ in 2015. Ten *Pseudo-nitzschia* species were 243 244 present in the GOM from 2012 to 2015, based on ARISA and sequencing data: P. pungens, P. plurisecta, P. seriata, and P. delicatissima were consistent members of the community, with 245 246 varying degrees of relative abundance, while P. multiseries, P. heimii/americana, P. fraudulenta, 247 P. cuspidata, P. caciantha, and P. obtusa were detected only in some years (Table 2). Before 2016, 248 GOM interannual variability was characterized by shifts in dominance between four species, but 249 not complete shifts in species assemblage. In addition, while some samples were dominated by 250 one species, in none of the years prior to 2016 was a single species dominant in all samples for 251 that year. 252 Seasonal Progression. Temporal variability also existed in the form of seasonal progression. Based 253 on the monitoring time series from MDIBL, there were two Pseudo-nitzschia cell concentration peaks in 2013 with varying species composition. The first peak of 150,000 cells L⁻¹ occurred in 254 255 late-July/early-August and was comprised largely of P. plurisecta (Figure 3). The second peak of

190,000 cells L⁻¹ occurred in mid-September and included mostly *P. pungens*.

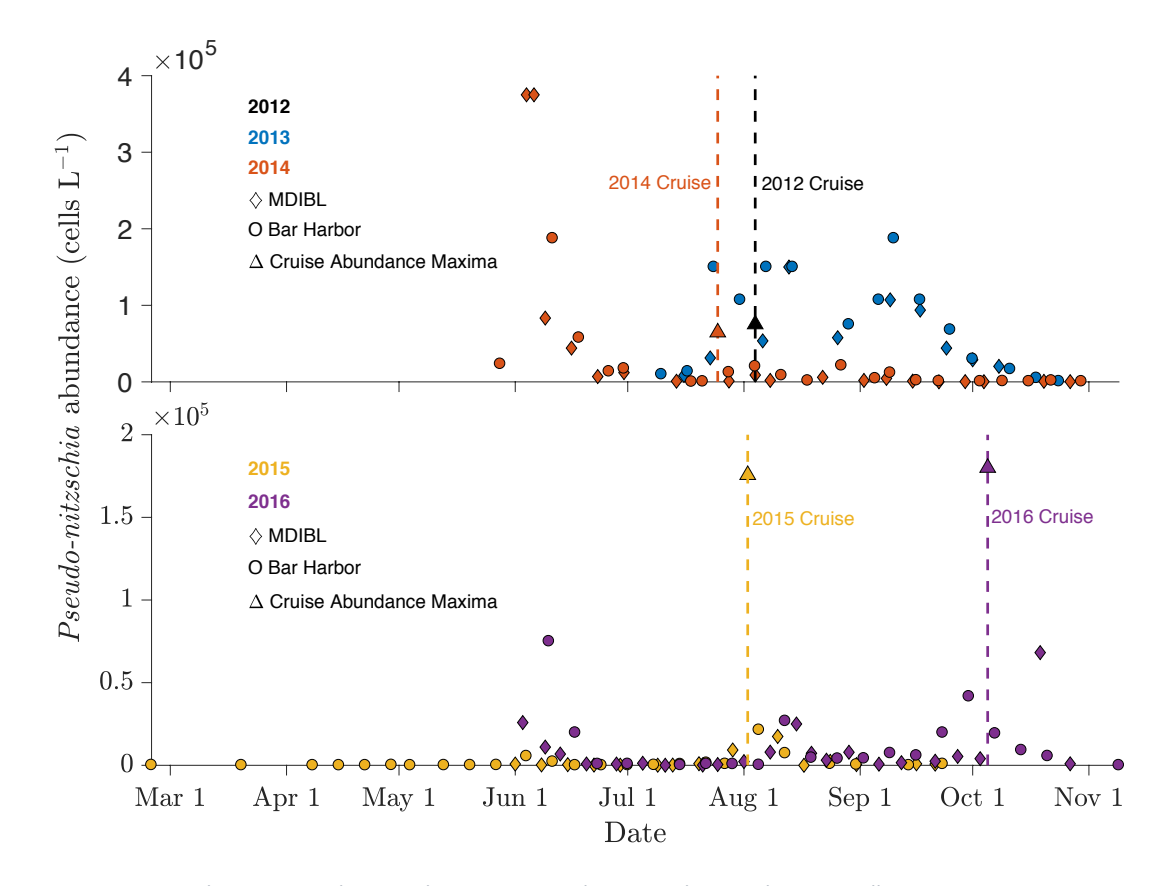


Figure 2 – From the MDIBL and Bar Harbor time series data, Pseudo-nitzschia spp. cell concentration versus time in 2013, 2014, 2015, and 2016. Timing of the 2014, 2015, and 2016 cruises are indicated with vertical lines. Maximum total cell abundance from each cruise is plotted as a single point. Note that the y axis scales are different.

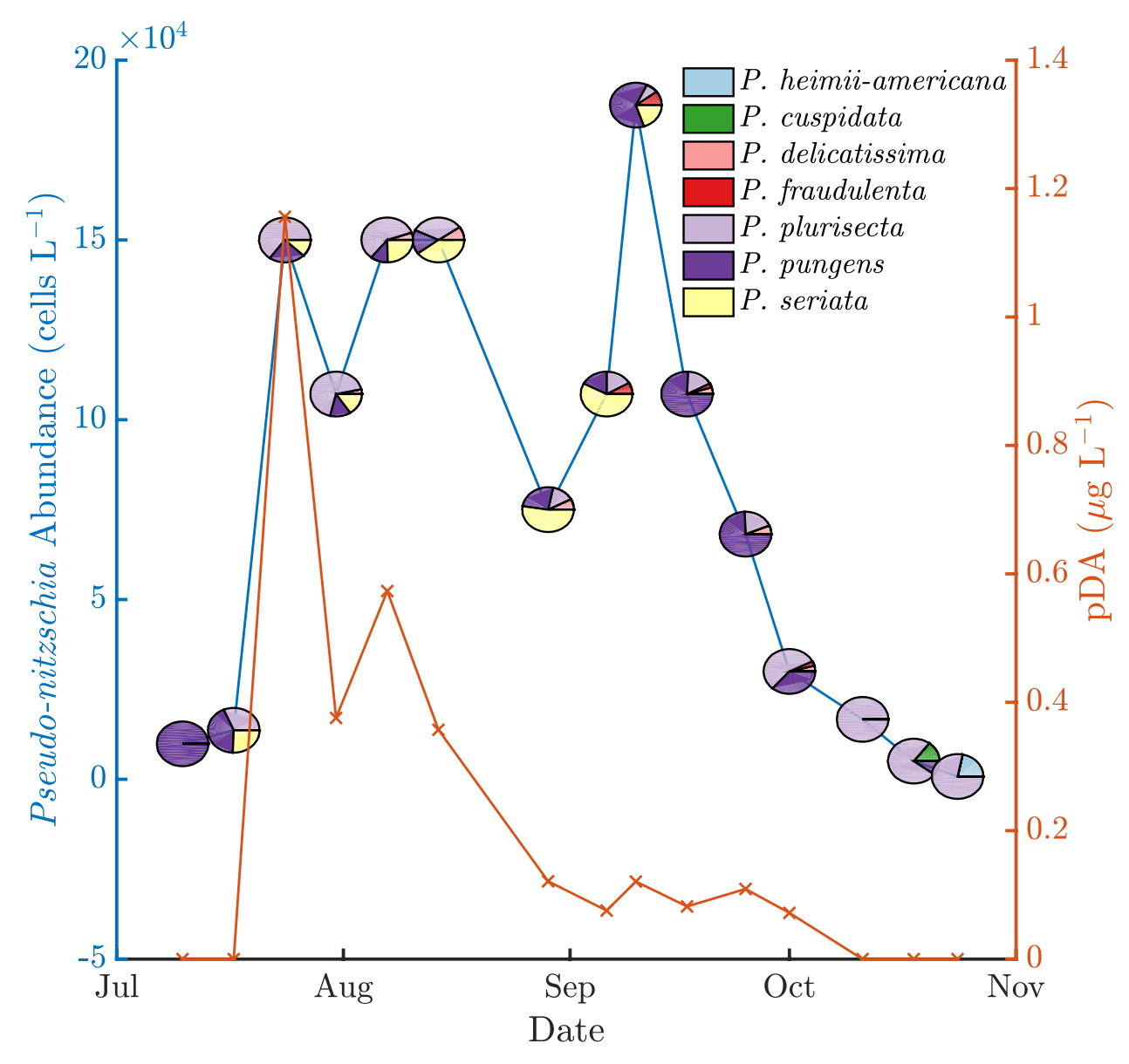


Figure 3 - From the Bar Harbor time series, Pseudo-nitzschia cell concentration (left axis; blue line) and pDA (right axis; red Xs) versus time in 2013. Relative species abundance for each sample is indicated with pie charts.

3.1.2 Spatial Variability

In addition to temporal variability, spatial variability was observed in the cruise data (Figure 4, Figure 5, Figure 6, and Figure 7). Prior to 2016, the greatest cell concentrations were consistently inshore and at the surface. Because the inshore waters also had lower salinity, the samples in 2012 and 2015 could be categorized into two groups: one group at higher salinity and lower cell counts (offshore), and the second group at lower salinities and higher cell counts (inshore).

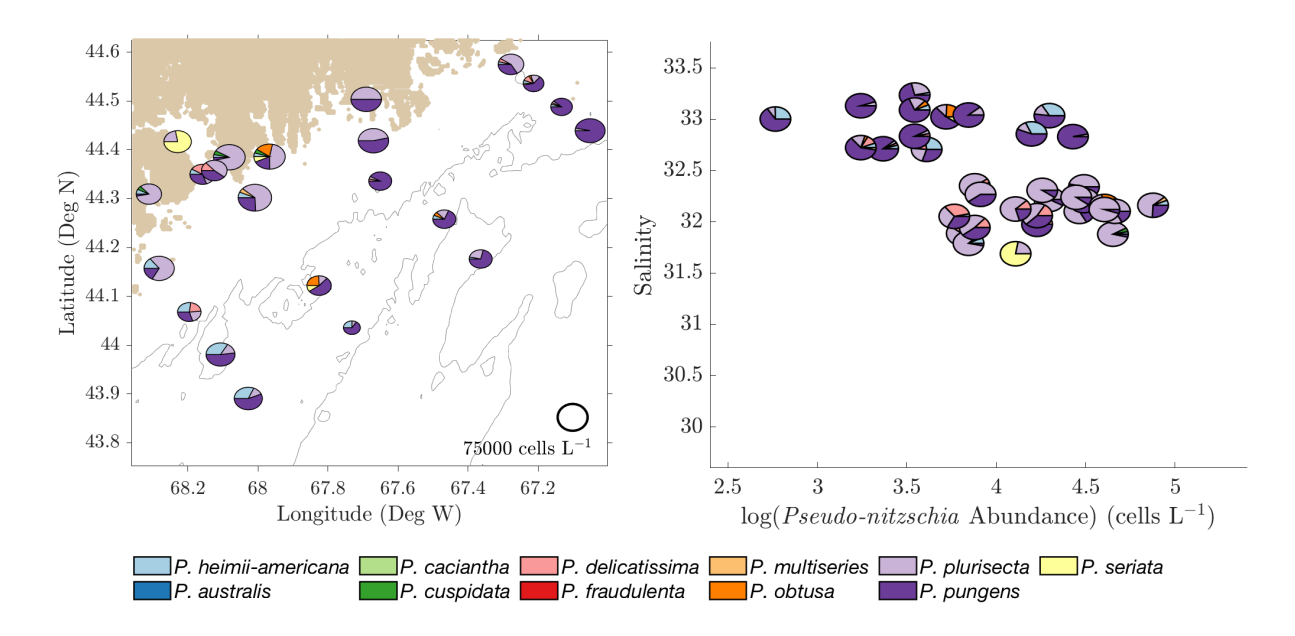


Figure 4 – (Left) August 2012 species relative abundance of surface samples plotted on the sampling locations in the GOM. Pie chart size was determined by log(cell count) (scale shown at lower right). (Right) 2012 relative species abundance on a salinity vs. cell count diagram, with axes scaled to match Figure 5, Figure 6, and Figure 7.

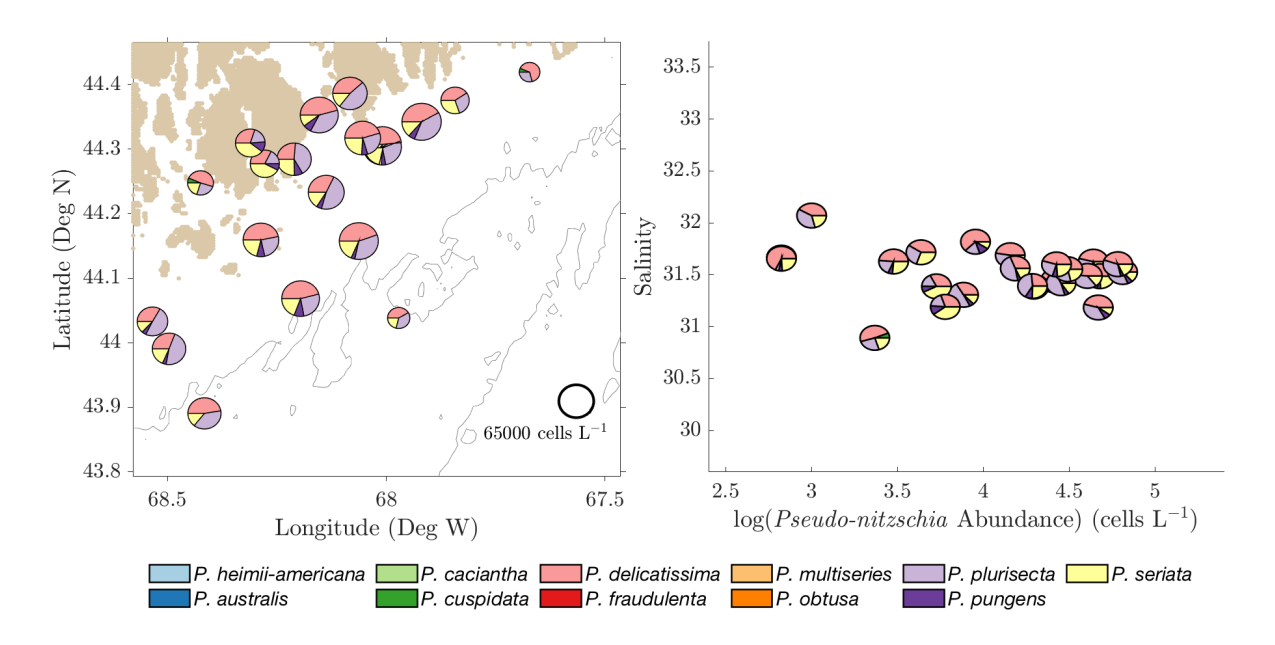


Figure 5 - (Left) July 2014 species relative abundance of surface samples plotted on the sampling locations in the GOM. Pie chart size was determined by log(cell count) (scale shown at lower right). (Right) 2014 relative species abundance on a salinity vs. cell count diagram, with axes scaled to match Figure 4, Figure 6, and Figure 7.

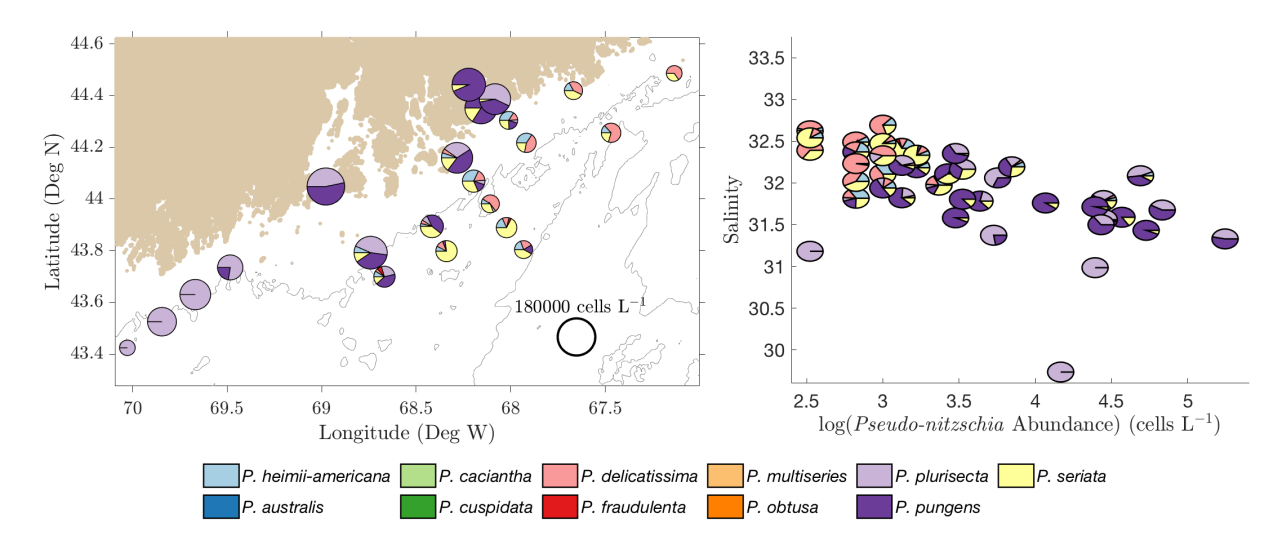


Figure 6 - (Left) August 2015 species relative abundance of surface samples plotted on the sampling locations in the GOM. Pie chart size was determined by log(cell count) (scale shown at lower right). (Right) 2015 relative species abundance on a salinity vs. cell count diagram, with axes scaled to match Figure 4, Figure 5, and Figure 7.

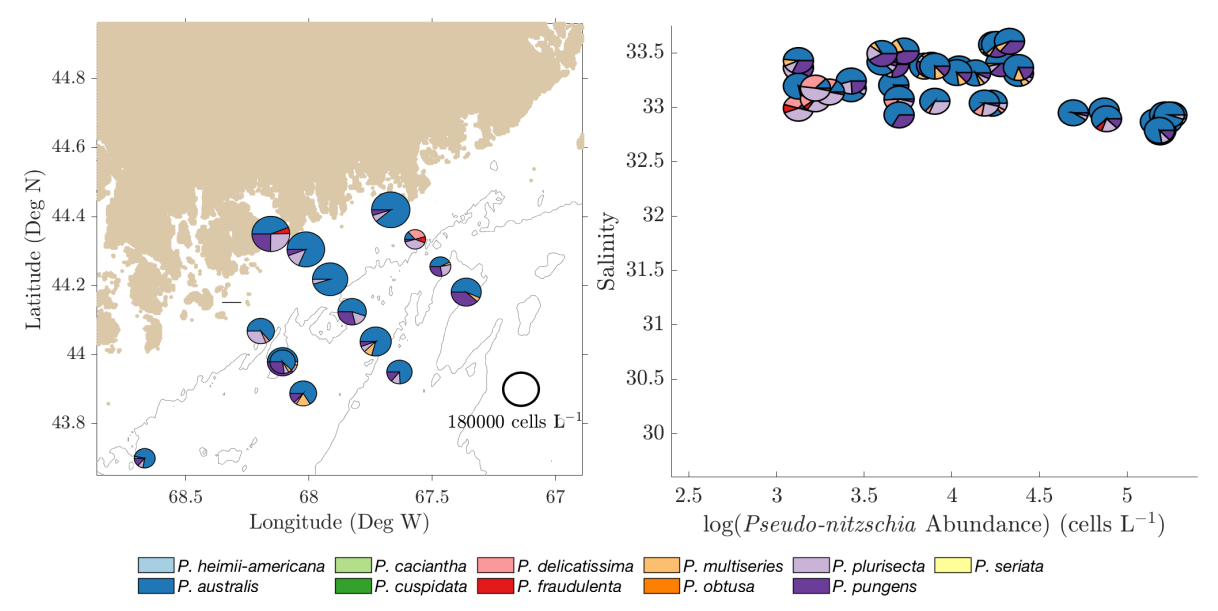


Figure 7 - (Left) October 2016 species relative abundance of surface samples plotted on the sampling locations in the GOM. Pie chart size was determined by log(cell count) (scale shown at lower right). (Right) 2016 relative species abundance on a salinity vs. cell count diagram, with axes scaled to match Figure 4, Figure 5, and Figure 6.

In 2012, inshore salinity ranged from 31.5 to 32.5 while offshore salinity ranged from 32.5 to 33.5 (Figure 4). In 2015, inshore salinity ranged from 29 to 32.5, while offshore salinity ranged from 32 to 33 (Figure 6). *P. plurisecta* was consistently found at greater relative abundance in inshore samples, while *P. seriata* and *P. delicatissima* were consistently found in offshore samples (Figure 4 and Figure 6). *P. pungens* was found both inshore and offshore.

3.2 2016 event

In 2016 shellfisheries were closed because shellfish DA concentrations exceeded the regulatory limit for the first time in the GOM (Bates et al., 2018). Particulate DA concentrations reached a maximum of 37.5 μ g L⁻¹ at one site and were on average an order of magnitude larger than pDA measured in previous years (Figure 8). Shellfishery closures in the GOM were preceded by shellfishery closures in the Bay of Fundy, where shellfish DA concentrations exceeded 20 μ g of DA g⁻¹ shellfish tissue at various locations from September 16 to 30 (Canadian Food Inspection Agency, 2016).

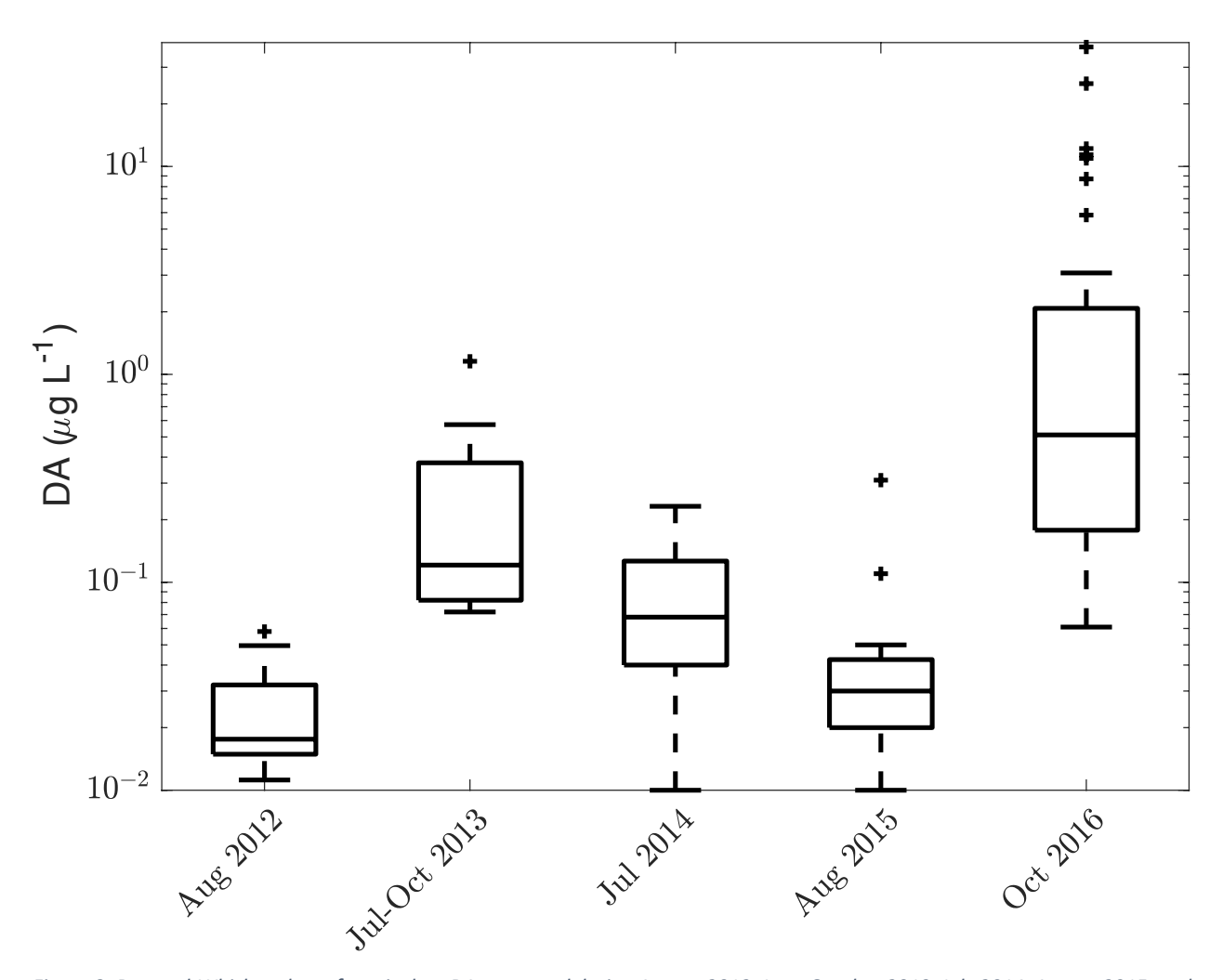


Figure 8- Box-and-Whisker plots of particulate DA measured during August 2012, June-October 2013, July 2014, August 2015, and October 2016. Note that the y axis is a log scale. The crosses are outliers, defined as points greater than (less than) Q3(Q1) +(-) 1.5*(Q3-Q1), where Q1 is the first quartile and Q3 is the third quartile.

The 2016 bloom likely began in September in the Bay of Fundy, and samples containing up to 180,000 *Pseudo-nitzschia* cells L⁻¹ were collected along the Eastern Maine coast during the 2016 cruise from October 5 to October 7. The bloom was accompanied by greater salinity, greater ammonium, and lower Si*, all of which were significantly different from measurements in at least one previous year (Section 3.4).

During the 2016 bloom, *P. australis* was observed at all sample sites and depths (Figure 7), and therefore at varying nutrient ratios and the full range of temperatures (12.23–14.20°C) and salinities (32.77–33.61) recorded that year. The inshore-offshore biogeographic patterns in cell abundance and species composition that were observed in summer 2012 and 2015 (Section 3.1) were not present in fall 2016. Cell abundances and *P. australis* relative abundance were relatively uniform across the sample area from inshore to offshore.

3.3 Domoic Acid

DA concentrations varied spatially, seasonally, and interannually, in correlation with cell concentrations and with the relative abundance of known toxic species (Figure 9). In 2012, the highest pDA (0.06 μ g L⁻¹) was observed in samples with at least 10⁴ cells L⁻¹ and >50% *P. plurisecta* relative abundance. At Mt. Desert Island in 2013, the first peak in cell abundance, which was dominated by *P. plurisecta*, a known toxic species, coincided with a peak in pDA (Figure 3). The second peak, however, which was dominated by *P. pungens*, did not result in elevated DA concentrations. In 2014, relative species proportions were constant, but pDA concentrations increased as absolute cell concentrations increased: the maximum pDA (0.23 μ g L⁻¹) co-occurred with a cell concentration of 15,000 cells L⁻¹, and most pDA concentrations over 0.1 μ g L⁻¹ co-occurred with cell concentrations greater than 10⁴ cells L⁻¹. In 2015, samples with *P. plurisecta* had higher pDA than those with *P. delicatissima* and *P. seriata*, and the greatest pDA concentration was 0.31 μ g L⁻¹. In 2016 the greatest pDA concentration was 37.5 μ g L⁻¹, and samples that were nearly completely dominated by *P. australis* had the greatest pDA.

Estimated cDA varied widely in the survey and time series data. From samples dominated by one species, cDA estimates were possible for *P. australis*, *P. pungens*, *P. seriata*, *P. delicatissima*, and

P. plurisecta. PDA was < LOQ in all samples dominated by *P. delicatissima*. Cellular DA estimates were < LOQ-11.1 pg cell $^{-1}$ for *P. seriata*, 0.6-26.7 pg cell $^{-1}$ for *P. plurisecta*, and 10.2-42.6 pg cell $^{-1}$ for *P. australis* (more information can be found in the supplementary material). *P. pungens* cDA estimates were only greater than zero when the analysis was run including samples with relative abundance as low as 60%, and ranged from <LOQ-0.75 pg cell $^{-1}$. This approach was validated by previously published estimates for the observed species: cDA estimates for *P. pungens* and *P. delicatissima* are less than 1 pg cell $^{-1}$, while cDA estimates for *P. seriata* range from 0.8-33.6 pg cell $^{-1}$ (Trainer et al., 2012). *P. plurisecta* was previously identified and confirmed to produce DA in the GOM (Fernandes et al., 2014), and *P. australis* cDA has been shown to reach > 90 pg cell $^{-1}$ (Ryan et al., 2017).

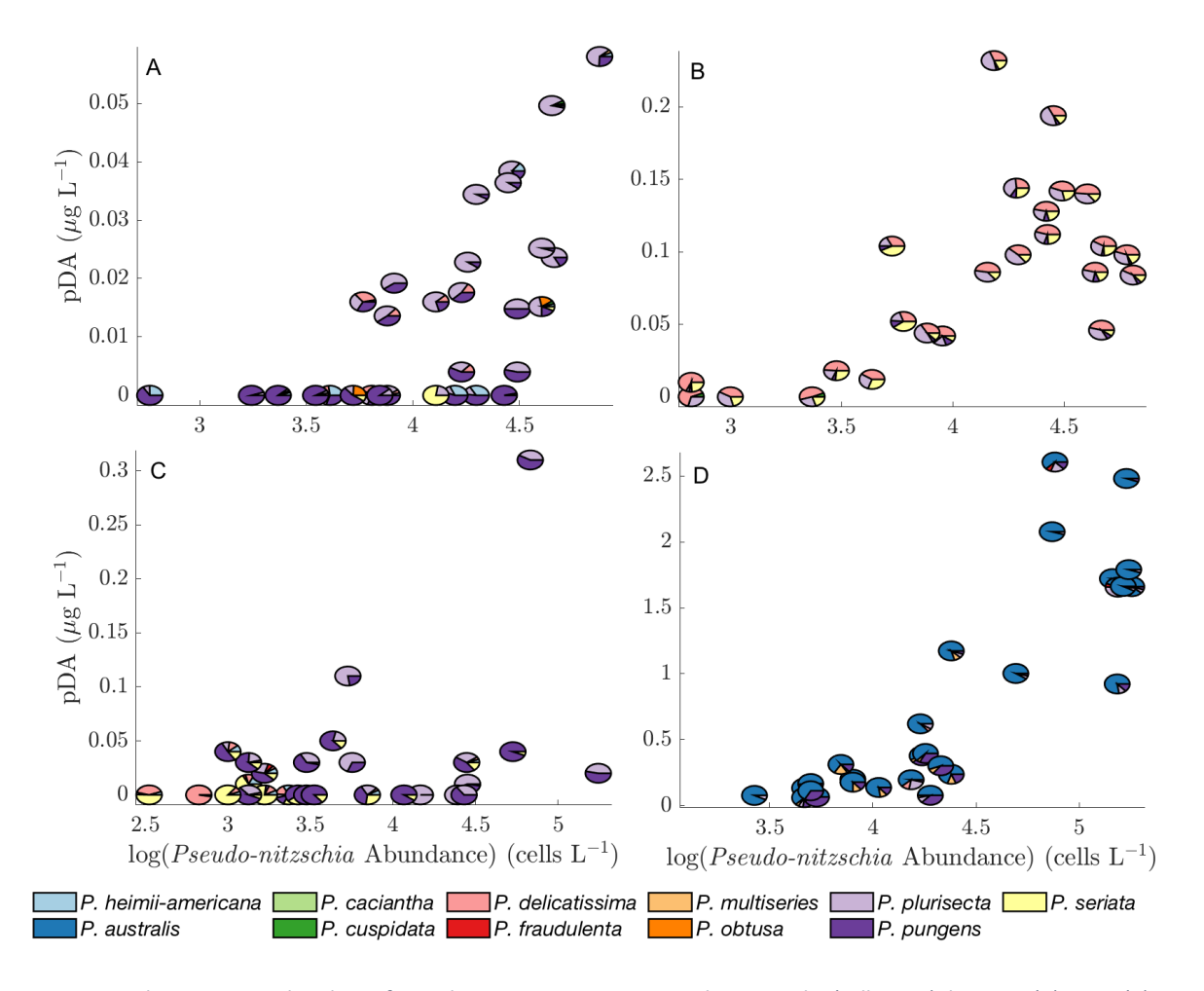


Figure 9 – Relative species abundance for each survey cruise on a particulate DA vs log(cell count) diagram: (A) 2012, (B) 2014, (C) 2015, (D) 2016. Note that the axes scales are not constant.

3.4 Statistical Analysis

344

345

346

347

348

349

350

351

352

353

354

355

356

357

358

359

360

361

362

363

364

365

366

367

368

369

370

except cDA.

Statistics were used to quantify correlations from the descriptive analysis, beginning with correlations with environmental parameters. Linear regressions between pDA concentrations or relative species abundance and environmental parameters yielded statistically significant results (p-value < 0.05), however the correlations were low (R² < 0.1). The exception is in linear regressions from 2013: P. pungens was negatively correlated with temperature (R² = 0.85), P. seriata was negatively correlated with salinity (R² = 0.53), and pDA was negatively correlated with phosphate (R² = 0.57). Some correlations existed between relative species abundance and salinity, which are discussed in Section 3.1.2. When the analysis included only samples with pDA > LOQ (130 out of 372 total samples), pDA and species abundance were not consistently correlated with one environmental parameter across the years. Thus, variabilities in species composition and pDA concentrations were not functions of any one environmental parameter. (Refer to supplementary material for full table of p-values and R² values from regression analysis.) Linear regressions between relative species abundance and pDA were similarly inconclusive: R² values were less than 0.2. Therefore one species was not the sole producer of pDA across all years of the study. However, when the analysis included only samples with pDA > LOQ, there were consistent correlations between pDA and the abundance of P. plurisecta, P. pungens, P. australis, and total cell counts (Table 3). CCA and PCA analyses were inconclusive: in neither of the analyses, whether each cruise individually or all cruises combined, were species clearly and consistently correlated with an environmental factor. From the analysis, nutrient and temperature variability dominated the system, but did not correlate with species variability. Despite a lack of direct correlations between environmental factors and species or pDA, interannual differences were observed. According to the Wilcoxon signed rank test, ammonium, N:P, and salinity were significantly higher in 2016 than in 2012 and 2015, while Si* and Si:N were significantly lower in 2016 compared to 2012 and 2015. 2016 was not significantly different from 2014 in any category

3.5 Physical Forcing and Hydrodynamics

The CUI in 2016 was at a minimum in May and increased faster in summer 2016 than in summer 2012, 2013, 2014, or 2015 (Figure 10). By late September 2016, the CUI was larger than in all previous years except 2013, and an abrupt shift to downwelling-favorable winds occurred from the 23rd to the 27th of September. Cumulative river discharge was lower than the average from the 2001–2015 climatology (supplementary materials), and salinities during the 2016 cruise were higher and had a narrower range than in previous cruises (Figure 10). North Atlantic inflows in 2016 were also noteworthy: at NERACOOS Station M in 2016 there was a warm and salty anomaly at 250 m that caused salinity to increase from 34.25 to 34.8 and temperature to increase from 8.71 to 10.35 °C in 6 days (Figure 11).

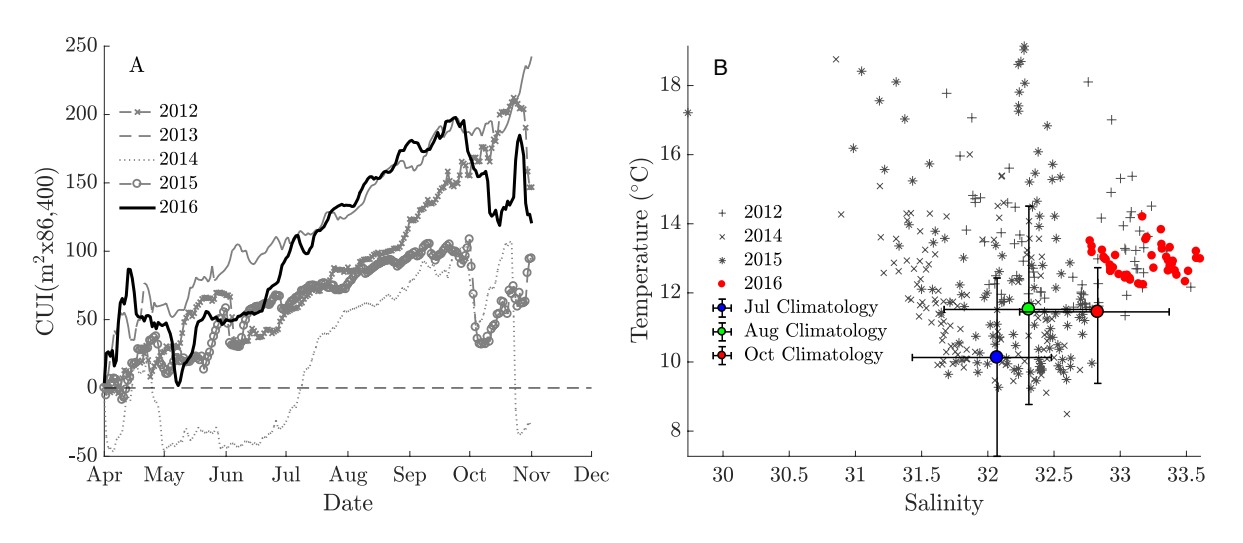


Figure 10- (A) Cumulative Upwelling Index vs time in 2012–2016, calculated with atmospheric data from NERACOOS Station I. (B) Temperature and salinity measurements from all ship surveys plotted on one temperature-salinity diagram. Climatological means (circles) and minima/maxima (error bars) of temperature and salinity for the months July, August, and October (the same months as the cruise surveys) are also shown from NERACOOS station I.

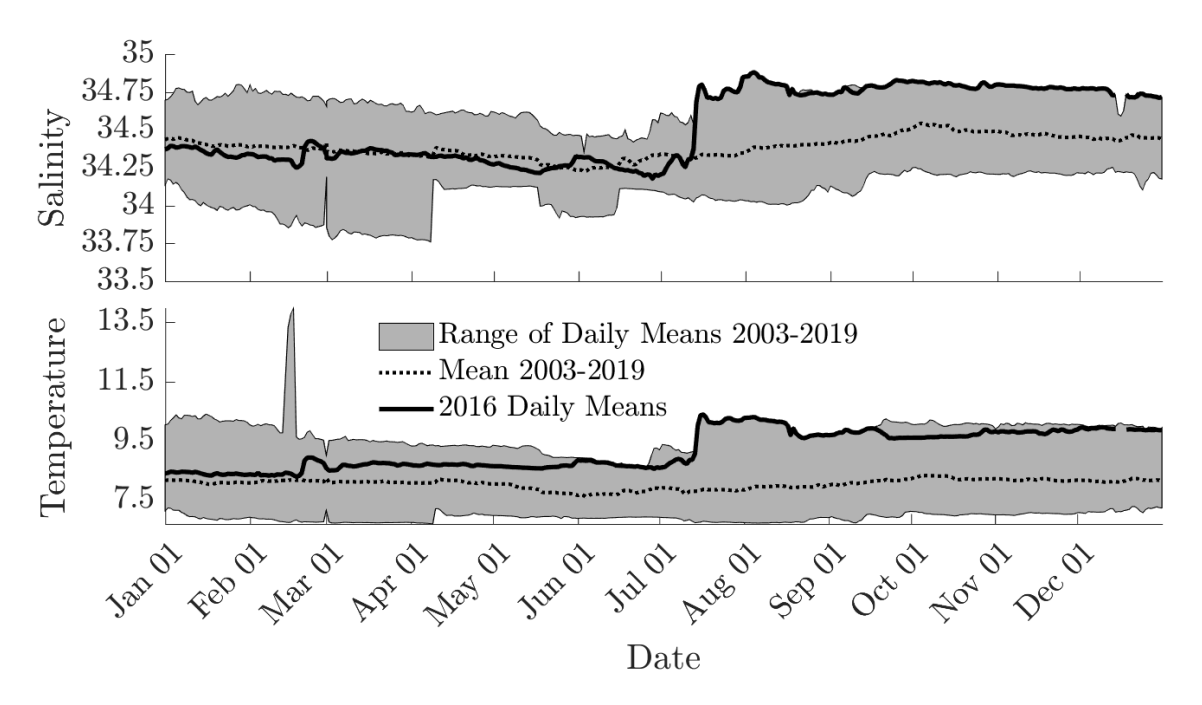


Figure 11 – Salinity (top) and temperature (bottom) climatology as measured by NERACOOS buoy station M (Jordan Basin) at 250m. Climatology was calculated from data measured in 2003–2019, and 2016 daily means are overlain.

4 Discussion

4.1 Pseudo-nitzschia Biogeography

Although inshore-offshore *Pseudo-nitzschia* biogeography correlated with salinity, it may not be due to differences in species' salinity preferences. In fact, the literature is inconsistent on salinity preferences for species in the dataset. For example, *P. delicatissima* and *P. pungens* were observed in salinities ranging from 20.8 to 38 in the western Mediterranean (Quijano-Scheggia et al., 2008), while a survey of the Bay of Seine (Thorel et al., 2017) found a trend that was the opposite: *P. pungens* was found in 32–33.5 salinity waters, while *P. delicatissima* was found in 31.6–32.8 salinity waters.

Cross-shore patterns could also be indicative of underlying water mass changes. For example, inshore-offshore patterns in species composition have been observed in Monterey Bay, where an upwelled cold tongue divided non-toxic inshore populations of *P. fraudulenta* from toxic offshore populations of *P. australis* (Bowers et al., 2018). In the GOM dataset, cross-shore patterns in species composition and salinity may reflect the coastal river plume decreasing salinity in the nearshore, which was apparent in 2012 (Figure 4) and in 2015 (Figure 6). If

variations in salinity are associated with different water masses, other factors likely varied simultaneously. Species' niche in salinity space was inconsistent from year to year in the GOM dataset, there are not currently enough data to tease apart the effects of only salinity from other factors, and seemingly contradictory findings in the literature may indicate intraspecific diversity. It is therefore not possible to define salinity niches in the GOM dataset.

4.2 Cruise Results in the Context of Temporal Variability

It may be tempting to draw conclusions about species' environmental preferences by comparing cruise data, but in each year the cruise data captured only a snapshot of a spatially and temporally variable process. It is therefore difficult to say what conditions preceded a bloom and how the bloom itself may have altered its environment. In addition, seasonal progression in species relative abundance (e.g. 2013, Figure 3) combined with interannual variability in the timing of peak cell abundance (Figure 2), make it unlikely that four different cruises conducted at different times captured the same point in the blooms' progression. Variations among years therefore cannot be used to draw conclusions about factors regulating species distribution.

In 2014, inshore-offshore patterns were less pronounced than in 2012 and 2015. One explanation for this is interannual variability in species dominance, which has also been observed in the Bay of Seine: a 2012 bloom was a composite of *P. australis, P. pungens,* and *P. fraudulenta,* but a 2013 bloom was dominated by *P. delicatissima* (Thorel et al., 2017). However, because the same species were present in the GOM in 2012, 2014, and 2015, but at varying relative abundances, it is more likely that the difference in biogeography is due to differences in cruise timing relative to bloom timing and seasonal cycles in environmental conditions. The 2014 survey occurred when Bar Harbor and MDIBL cell concentrations were low, and *P. plurisecta* was observed in similar proportions across most sample sites. The 2012 and 2015 cruises, meanwhile, occurred when cell concentrations were at a maximum, and *P. plurisecta* dominated inshore (Figure 2). In 2013, species assemblage shifted from a more even distribution early in the season to dominance by *P. plurisecta* later in the season (Figure 3). Similar seasonal transitions have been observed in the English Channel (Downes-Tettmar et al., 2013) and western Scottish waters (Fehling et al., 2006): multiple species existed at one location, but they bloomed at different times of the year.

Assuming the temporal pattern observed in the 2013 time series was consistent for the years preceding 2016, the cruises likely captured inshore summertime *P. plurisecta* dominance in 2012 and 2015 but not in 2014.

4.3 Domoic Acid

The production of DA in the ocean depends both on the presence/abundance of a toxic species and on conditions that lead to DA synthesis. Genetic analysis confirmed the presence of certain species and pDA in each of the sampling years: *P. plurisecta* and *P. seriata* from 2012–2015, and *P. plurisecta*, *P. seriata*, and *P. australis* in 2016. In the cruise samples and MDIBL time series pDA typically increased with increasing relative abundance of *P. plurisecta* and *P. australis*, known DA-producers (Figure 3 and Figure 9). In 2016, when the species assemblage was dominated by the putatively toxic *P. australis*, pDA levels were an order of magnitude higher than previous years. In samples where pDA > LOQ, pDA was correlated with *P. pungens*, *P. plurisecta*, *P. australis* and total cell counts. Cellular DA calculations varied between species (Section 3.3), with highest cDA estimates for *P. australis* cells, followed by *P. plurisecta*, and finally *P. seriata* and *P. pungens*. Particulate DA concentrations were correspondingly highest in *P. australis*-dominated samples, followed by *P. plurisecta* samples, and *P. seriata* samples.

The effect of species composition on DA concentrations is supported by studies in both the field and the lab. In the Bay of Seine, Thorel et al., (2017) observed that blooms dominated by *P. delicatissima* were non-toxic, while blooms dominated by *P. australis* were toxic. That study reported variability in species composition, nutrient concentrations, nutrient ratios, salinity, temperature, and irradiance, but concluded that, of all these, species composition had the largest effect on DA. Similarly, Downes-Tettmar et al. (2013) observed seasonal variations in DA and species composition in the Western English Channel and concluded that DA concentrations correlated with cells from the *P. seriata* group (of which *P. australis* is part) and *P. pungens/multiseries* group. Lab studies have led to similar conclusions. Lema et al. (2017) measured the effects of varying phosphorus concentrations and changing species composition on DA production and concluded that species was the leading order factor to DA production.

Based on cDA analysis, linear regressions, and evidence from the literature, species composition was likely the leading factor affecting pDA concentrations in the GOM.

The presence of toxic Pseudo-nitzschia spp. is not the only factor for pDA concentrations, as production of DA can vary depending on life stage (Auro and Cochlan, 2013), light availability (Auro and Cochlan, 2013; Terseleer et al., 2013), macronutrients (Lema et al., 2017), nutrient ratios (Lema et al., 2017), trace metals (Wells et al., 2005), or even the presence/absence of predatory zooplankton (Lundholm et al., 2018; Tammilehto et al., 2015). The Wilcoxon signedrank test indicated that Si:N of positive DA samples was significantly lower in 2016 than in 2012 and 2015, and that N:P was significantly higher in 2016 than in 2012 or 2015. This may be the result of the significantly higher ammonium concentrations that were measured in 2016, because, in the ratios, N was the sum of NO_x and NH⁴⁺. However, Si* was also significantly lower in 2016, and that measurement is only a comparison between Si(OH)₄ and NO_x. Several lab studies have found DA production to increase under silicic acid-limiting conditions when nitrogen was abundant (Lema et al., 2017; Tatters et al., 2012; Terseleer et al., 2013). One field study also observed that maximum pDA concentrations occurred when both silicate and phosphate were limiting (Thorel et al., 2017). Although this ratio was not directly correlated with pDA concentrations in the present study, its role in triggering and enhancing DA production by P. australis and other species cannot be ignored.

Despite the laboratory evidence of the role of environmental factors in DA production, it is difficult to translate lab results to the field. Communities in the lab are often monospecific, and all other factors besides the parameter in question are carefully controlled. In the field, there are typically many *Pseudo-nitzschia* species present as well as other plankton that interact with *Pseudo-nitzschia* and utilize nutrients. For example, grazer interactions have recently been shown to dramatically enhance DA production in *Pseudo-nitzschia* (Lundholm et al., 2018). As in this study, studies along the Washington and California coasts were unable to attribute DA concentrations or species abundance to a single environmental parameter (Smith et al., 2017; Trainer et al., 2009). The lack of simple correlations between environmental factors and pDA

does not indicate that environmental factors are unimportant, but rather that pDA concentrations in the field likely depend on a combination of many different factors.

4.4 The 2016 Event

The DA event in 2016 was unique from previous years in three ways. First, *P. australis* was identified for the first time in the GOM (Bates et al., 2018). Second, the bloom occurred in September and October, whereas in previous years *Pseudo-nitzschia* cell concentrations peaked in the spring or summer (Figure 3 and Figure 4) and the bloom season had been assumed to end in fall. Third, the species assemblage during the 2016 bloom was not a mix of *P. delicatissima*, *P. seriata*, *P. plurisecta*, and *P. pungens*, but rather dominated by one species. *P. australis* was present in every sample, and in many samples its relative abundance was more than 50% by ARISA estimates.

4.4.1 What Caused the abnormally high pDA levels in 2016?

The historic shellfish closures in the GOM in 2016 prompt the question: why was pDA so high?

PDA values in 2016 were likely the result of high *P. australis* relative abundance in combination
with limiting silicic acid concentrations, but, of these, *P. australis* was the leading order factor in high pDA levels.

P. australis is one of the most toxic *Pseudo-nitzschia* species, both in this dataset and in the literature (Section 4.3). The presence of *P. australis* alone might be enough to explain the high pDA levels in 2016, because cDA was significantly higher in 2016 despite similar total cell counts. However, significantly lower Si* co-occurred with the *P. australis* cells in 2016, and DA production has been linked to silica stress in both the laboratory (Doucette et al., 2008; Terseleer et al., 2013), and the field (Marchetti et al., 2004; Ryan et al., 2017). Low Si* may have enhanced DA production by *P. australis* cells to create higher pDA concentrations. Because 2014 had equally low Si* to 2016 but pDA concentrations in line with 2012, 2013, and 2015, and since *P. australis* was not present in 2014, *P. australis* was probably the leading factor for the high pDA concentrations in 2016.

4.4.2 Where did *P. australis* originate?

The first hypothesis for the origin of *P. australis* is that it was present in undetectable amounts prior to 2016 and grew in 2016 because of altered environmental conditions. This hypothesis cannot be ruled out, but it seems unlikely, because there is little evidence to suggest that there were sufficient changes to growth conditions to favor a P. australis bloom. Nutrient concentrations and ratios were not significantly different in 2016 compared to all prior years. Si* was significantly lower in 2016 compared to 2012 and 2015, but this is expected to stress Pseudonitzschia cells, not improve their growth (Terseleer et al., 2013). There is no evidence in the literature to suggest that P. australis growth in particular improves with low silicic acid, so it is unknown whether low Si* might have enhanced P. australis growth over other Pseudo-nitzschia species. NH₄⁺ was significantly higher in 2016 compared to 2012 and 2015, and in Puget Sound P. australis and P. seriata relative abundance were found to correlate with NH₄+ (Hubbard et al., 2014), but growth experiments have not found significantly improved *P. australis* growth when nitrogen was in the NH₄⁺ form (Howard et al., 2007; Martin-Jézéquel et al., 2015). As previously discussed, it is difficult to draw conclusions about the conditions preceding a bloom from survey data alone. Thus, the differences in nutrients in 2016 do not conclusively point to improved conditions for *P. australis* growth.

Salinity was significantly higher in 2016 than in three previous years, suggesting a possible factor in the emergence of *P. australis*. It is possible for salinity to favor *P. australis* growth, because *P. australis* has been shown to prefer a more limited range of salinity relative to other species (Ayache et al., 2018), but the 2016 cruise data are insufficient to fully explore correlations between *P. australis* and salinity. The greater salinity values in 2016 compared to those in previous years (Figure 10) could be explained in a number of ways, some of which point to other explanations for the *P. australis* bloom. The 2016 cruise occurred later in the year than previous years, and salinity typically increases through the summer and fall in the GOM. Salinity during the 2016 cruise was only slightly higher than regional climatology for that time of year (Figure 10). Relatively low river discharge in 2016 also may have led to greater than average salinities inshore (supplementary material).

The high salinity values may also indicate an anomalous water mass, which relates to a hypothesis that P. australis was introduced into the GOM in 2016. Inflows from the Scotian Shelf and Northeast Channel vary in strength interannually (Townsend et al., 2014), and may provide a potential pathway for introducing P. australis cells. In particular, climatology from NERACOOS station M in Jordan Basin showed a rapid increase in salinity and temperature values in summer 2016 at 250 m (Figure 11) that may have been associated with anomalously warm/salty eddies propagating from the Grand Banks near Novia Scotia (Brickman et al., 2018) or with Gulf Stream Ring water (GSRW). Townsend et al., (2015) showed evidence of GSRW, or a mixture containing a significant fraction of GSRW, that had penetrated at intermediate and bottom depths into Jordan Basin in the interior GOM in the fall of 2013. They analyzed a time series of temperature and salinity at Buoy M in Jordan Basin, as augmented by in situ nitrate data collected at 100 m with a Satlantic optical nitrate sensor (Twardowski et al., 2015). Nitrate served as a third semiconservative water mass tracer to identify an intrusion of anomalously warm and salty, but low nitrate, GSRW. Unlike low-nitrate GSRW, an intrusion of Warm Slope Water with similar T/S properties would have exhibited elevated nitrate concentrations (typically 16-17 μ M; Townsend et al. 2006), not the drop from 12 μ M to 8 μ M that was observed (Townsend et al., 2015).

Similarly timed signals were observed at buoy station M in Jordan Basin in 2016 and in the late summer and fall in 2017 and 2018. Deep waters (at 200 m and 250 m) during those events exhibited the warmest and saltiest values of the time series in Jordan Basin (2003 to present) and were accompanied by lowered nitrate concentrations (Townsend, unpubl.), characteristic of GSRW (Townsend et al., 2010). Warm Core Rings can encompass 1500m in the vertical (Joyce, 1984) which suggests that the signals observed at 250m in 2016 and 100m in 2013 (Townsend et al., 2015) could both have been caused by GSRW.

From GOM hydrodynamics, bloom timing, and experiments in *Pseudo-nitzschia* physiology, it is plausible that the *P. australis* cells observed in the Bay of Fundy and near eastern Maine in 2016 were carried in with a GSRW intrusion. The intrusion was observed in Jordan Basin in July. Assuming an average current speed of 10 cm s⁻¹, it would have taken one to two months for this water to circulate the basin and transit to the Bay of Fundy, where elevated DA concentrations

led to shellfishery closures in early September 2016. Therefore, there was more than enough time for the water mass to advect to the bloom region, where it would be mixed into the upper water column by strong tidal pumping in those areas. Notably, this would also require a departure from the climatological circulation pictured in Figure 1, which is possible in the event of an anomalous water mass intrusion. Because the anomaly in Jordan Basin was observed at 250 m, any *Pseudo-nitzschia* cells associated with this water mass would have been deep in the water column, and a question remains whether the cells can survive at depth for an extended period of time. In a recent experiment, *Pseudo-nitzschia* spp. cultures (species not specified) were able to survive more than 6 weeks of complete darkness and resume growth with no lasting effects (Fang and Sommer, 2017).

Continuous plankton recorder (CPR) data from offshore and from on the Scotian Shelf in 2016 were examined to look for offshore peaks in large *Pseudo-nitzschia* cell concentrations, but none were found (refer to supplementary material for plots of CPR data). This does not completely rule out the North Atlantic as a source, however, because the CPR data had coarse temporal resolution and samples were only taken from the surface, so sub-surface populations would not have been detected. The intrusion hypothesis can therefore be neither refuted nor confirmed, and remains a possibility.

4.4.3 Hydrodynamics as drivers of the 2016 bloom

The cumulative upwelling index (CUI) gave important clues to the timing of the 2016 *P. australis* bloom. Wind direction has been shown to influence alongshore transport in the GOM: in 2010, strong upwelling-favorable winds in combination with a weak dynamic height gradient led to weak alongshore flow, reducing the alongshore extent of an *A. catenella* bloom (McGillicuddy et al., 2011). In 2016 the CUI began at a minimum in May and rapidly climbed to outpace every other year except 2013 (Section 3.5). Upwelling-favorable winds in 2016 may have reduced alongshore transport and led to *Pseudo-nitzschia* retention in the Bay of Fundy, where DA in excess of 20 μ g g⁻¹ of shellfish tissue was recorded from September 16–30 (Canadian Food Inspection Agency).

A rapid switch from upwelling-favorable to downwelling-favorable winds occurred from September 23rd to 27th, potentially accelerating alongshore flow and cell transport (Franks and Anderson, 1992). Shellfish closure timing aligned with alongshore transport time: shellfisheries in Cobscook Bay on the Canadian border were closed on September 27th, 2016, and shellfisheries at Mt. Desert Island 95 km away were closed 3 days later, on September 30th, 2016 (Rappaport, 2016). In addition, there were recalls of mussels and mahogany quahogs harvested near Jonesport, ME between September 25 and 30 and clams harvested near Corea, ME between September 28 and 30. From NERACOOS buoy I, the average surface current speed in 2016 was 0.3 m s⁻¹. Assuming this average, it would take less than a day for alongshore currents to transport cells from the Bay of Fundy to Cobscook Bay, and about 4 days for them to transport cells to Mt. Desert Island. These timelines and calculations are estimates, but they suggest that the shift from upwelling-favorable to downwelling-favorable winds on September 23rd–27th was a factor in bloom timing on the coast of Maine.

5 Conclusion

This paper builds on the work of Fernandes et al. (2014) by analyzing the spatial and temporal patterns in *Pseudo-nitzschia* species composition in the GOM. ARISA was used to identify 11 species from ship survey and time series samples in 2012, 2013, 2014, 2015, and 2016. Pre-2016, observed *Pseudo-nitzschia* blooms followed consistent biogeography in the GOM, with *P. plurisecta* inshore and *P. seriata* and *P. delicatissima* offshore. In addition, pDA concentrations increased with cell concentrations, toxic species relative abundance, and as a result of interspecies variation in cellular DA quotas.

Spatial, seasonal, and interannual variability in species composition and absolute cell abundance may have been influenced by seasonal and interannual variations in upwelling winds, North Atlantic inflows, cumulative river discharge, and alongshore transport. The effects of these regional patterns may have been modified by local variations in temperature, salinity, nutrient concentrations, and nutrient ratios, but in contrast to several other studies (e.g., Kaczsmarska et al. 2007) no significant correlations between individual species and environmental factors, individual species and pDA, or environmental factors and pDA were found. Increased relative

abundance of toxic species led to increased pDA, but DA concentrations were likely caused by a combination of species composition and environmental factors.

Of particular interest was the 2016 P. australis bloom. This was the first known observation of P. australis in the GOM, and it was the first time in GOM history that shellfisheries were closed because DA concentrations exceeded the regulatory limit (Bates et al., 2018). Particulate DA concentrations reached 37.5 μ g L⁻¹ in 2016, which is comparable in magnitude to DA that has been measured on the west coast of the U.S. during Pseudo-nitzschia blooms. The high pDA in 2016 is attributed to the presence of P. australis in combination with low Si*. The source of P. australis is still unclear; we hypothesize that the species was carried in on an anomalous water mass in 2016, but more investigation is needed to determine the origin of these toxic cells, as well as the extent to which they persist within the GOM. Continued monitoring is essential both to improve the understanding of Pseudo-nitzschia bloom dynamics in the GOM and for the protection of public health.

6 Acknowledgements

This research was funded by the National Science Foundation (Grant Numbers OCE-1314642 and OCE-1840381), the National Institute of Environmental Health Sciences (Grant Numbers 1P01ES021923-01 and P01 ES028938-01), the Woods Hole Center for Oceans and Human Health, the Academic Programs Office of the Woods Hole Oceanographic Institution, and National Oceanic and Atmospheric Administration's HAB Event Response Program (2012 and 2016). We thank Maura Thomas at the University of Maine for support with nutrient collection and analysis. We also thank Kohl Kanwit at the Maine Department of Marine Resources, Anna Farrell, Jane Disney, and Hannah Mogenson at the Mt. Desert Island Biological Laboratory, Steve Archer at Bigelow Laboratory for Ocean sciences, and Bruce Keafer at the Woods Hole Oceanographic Institution for their work collecting samples and data used in the study. We also thank Maya Robert, Christina Chadwick, Laura Markley, Stephanie Keller Abbe, Karen Henschen, Emily Olesin, Steven Bruzek, Sheila O'Dea, April Granholm, Leanne Flewelling, and Elizabeth Racicot at the Florida Fish and Wildlife Conservation Commission-Fish and Wildlife Research Institute for processing samples for DA, DNA-based analyses, and cellular abundance.

551 552	7 Bibliography Anderson, C.R., Brzezinski, M.A., Washburn, L., Kudela, R., 2006. Circulation and environmental
553	conditions during a toxigenic Pseudo-nitzschia australis bloom in the Santa Barbara
654	Channel, California. Mar. Ecol. Prog. Ser. 327, 119–133.
555	Auro, M.E., Cochlan, W.P., 2013. Nitrogen Utilization and Toxin Production by Two Diatoms of
556	the Pseudo-nitzschia pseudodelicatissima Complex: P. cuspidata and P. fryxelliana. J.
557	Phycol. 49, 156–169. https://doi.org/10.1111/jpy.12033
558	Ayache, N., Hervé, F., Martin-Jézéquel, V., Amzil, Z., Caruana, A.M.N., 2018. Influence of sudden
559	salinity variation on the physiology and domoic acid production by two strains of Pseudo-
560	nitzschia australis. J. Phycol. 33, 0–3. https://doi.org/10.1111/jpy.12801
561	Bates, S.S., Bird, C.J., de Freitas, A.S.W., Foxall, R., Gilgan, M., Hanic, L.A., Johnson, G.R.,
562	McCulloch, A.W., Odense, P., Pocklington, R., Quilliam, M.A., Sim, P.G., Smith, J.C., Subba
563	Rao, D.V., Todd, E.C.D., Walter, J.A., Wright, J.L.C., 1989. Pennate Diatom Nitzschia
564	pungens as the Primary Source of Domoic Acid, a Toxin in Shellfish from Eastern Prince
665	Edward Island, Canada. Can. J. Fish. Aquat. Sci. 46, 1203–1215.
566	https://doi.org/10.4224/23000873
567	Bates, S.S., Hubbard, K.A., Lundholm, N., Montresor, M., Leaw, C.P., 2018. Pseudo-nitzschia,
568	Nitzschia, and domoic acid: New research since 2011. Harmful Algae 79, 3–43.
569	https://doi.org/10.1016/j.hal.2018.06.001
570	Bisagni, J.J., Gifford, D.J., Ruhsam, C.M., 1996. The spatial and temporal distribution of the
571	Maine Coastal Current during 1982. Cont. Shelf Res. 16, 1–24.
572	Bowers, H.A., Ryan, J.P., Hayashi, K., Woods, A.L., Marin, R., Smith, G.J., Hubbard, K.A.,
573	Doucette, G.J., Mikulski, C.M., Gellene, A.G., Zhang, Y., Kudela, R.M., Caron, D.A., Birch,
674	J.M., Scholin, C.A., 2018. Diversity and toxicity of Pseudo-nitzschia species in Monterey
675	Bay: Perspectives from targeted and adaptive sampling. Harmful Algae 78, 129–141.
676	https://doi.org/10.1016/j.hal.2018.08.006
677	Bresnan, E., Kraberg, A., Fraser, S., Brown, L., Hughes, S., Wiltshire, K.H., 2015. Diversity and
578	seasonality of Pseudo-nitzschia (Peragallo) at two North Sea time-series monitoring sites.
579	Helgol. Mar. Res. 69, 193–204. https://doi.org/10.1007/s10152-015-0428-5

680 Brickman, D., Hebert, D., Wang, Z., 2018. Mechanism for the recent ocean warming events on 681 the Scotian Shelf of eastern Canada. Cont. Shelf Res. 156, 11–22. 682 https://doi.org/10.1016/j.csr.2018.01.001 683 Canada, E., 2018. Water Level and Flow [WWW Document]. 684 Cusack, C., Mouriño, H., Moita, M.T., Silke, J., 2015. Modelling Pseudo-nitzschia events off 685 southwest Ireland. J. Sea Res. 105, 30-41. https://doi.org/10.1016/j.seares.2015.06.012 686 Doucette, G.J., King, K.L., Thessen, A.E., Dortch, Q., 2008. The effect of salinity on domoic acid 687 production by the diatom Pseudo-nitzschia multiseries. Nov. Hedwigia 133, 31–46. 688 Downes-Tettmar, N., Rowland, S., Widdicombe, C., Woodward, M., Llewellyn, C., 2013. 689 Seasonal variation in Pseudo-nitzschia spp. and domoic acid in the Western English 690 Channel. Cont. Shelf Res. 53, 40–49. https://doi.org/10.1016/j.csr.2012.10.011 691 Fang, X., Sommer, U., 2017. Overwintering effects on the spring bloom dynamics of 692 phytoplankton. J. Plankton Res. 39, 772-780. https://doi.org/10.1093/plankt/fbx046 693 Fehling, J., Davidson, K., Bolch, C., Tett, P., 2006. Seasonality of Pseudo-nitzschia 694 spp.(Bacillariophyceae) in western Scottish waters. Mar. Ecol. Prog. Ser. 323, 91–105. 695 Fehling, J., Green, D.H., Davidson, K., Botch, C.J., Bates, S.S., 2004. Domoic acid production by 696 Pseudo-nitzschia seriata (bacillariophyceae) in Scottish waters. J. Phycol. 40, 622–630. 697 https://doi.org/10.1111/j.1529-8817.2004.03200.x 698 Fernandes, L.F., Hubbard, K.A., Richlen, M.L., Smith, J., Bates, S.S., Ehrman, J., Léger, C., Mafra, 699 L.L., Kulis, D., Quilliam, M., Libera, K., McCauley, L., Anderson, D.M., 2014. Diversity and toxicity of the diatom Pseudo-nitzschia Peragallo in the Gulf of Maine, Northwestern 700 701 Atlantic Ocean. Deep. Res. Part II Top. Stud. Oceanogr. 103, 139–162. 702 https://doi.org/10.1016/j.dsr2.2013.06.022 703 Franks, P.J.S., Anderson, D.M., 1992. Marine Biology in a buoyancy current: Alexandrium 704 tamarense in the Gulf of Maine. Mar. Biol. 112, 153-164. 705 Guannel, M.L., Haring, D., Twiner, M.J., Wang, Z., Noble, A.E., Lee, P.A., Saito, M.A., Rocap, G., 706 2015. Toxigenicity and biogeography of the diatom Pseudo-nitzschia across distinct 707 environmental regimes in the South Atlantic Ocean. Mar. Ecol. Prog. Ser. 526, 67–87.

708

https://doi.org/10.3354/meps11027

- 709 Hansen, L.R., Soylu, S. í, Kotaki, Y., Moestrup, Ø., Lundholm, N., 2011. Toxin production and 710 temperature-induced morphological variation of the diatom Pseudo-nitzschia seriata from 711 the Arctic. Harmful Algae 10, 689-696. https://doi.org/10.1016/j.hal.2011.05.004 712 Hasle, G.R., 2002. Are most of the domoic acid-producing species of the diatom genus Pseudo-713 nitzschia cosmopolites? Harmful Algae 1, 137-146. https://doi.org/10.1016/S1568-714 9883(02)00014-8 715 Howard, M.D.A., Cochlan, W.P., Ladizinsky, N., Kudela, R.M., 2007. Nitrogenous preference of 716 toxigenic Pseudo-nitzschia australis (Bacillariophyceae) from field and laboratory 717 experiments. Harmful Algae 6, 206-217. https://doi.org/10.1016/j.hal.2006.06.003 718 Hubbard, K.A., Olson, C.E., Armbrust, E.V., 2014. Molecular characterization of Pseudo-nitzschia 719 community structure and species ecology in a hydrographically complex estuarine system 720 (Puget Sound, Washington, USA). Mar. Ecol. Prog. Ser. 507, 39–55. 721 https://doi.org/10.3354/meps10820 722 Joyce, T.., 1984. Velocity and Hydrographic Structure of a Gulf Stream Warm-Core Ring. J. Phys. 723 Oceanogr. 14, 936–947. 724 Keafer, B.A., Churchill, J.H., McGillicuddy, D.J., Anderson, D.M., 2005. Bloom development and 725 transport of toxic Alexandrium fundyense populations within a coastal plume in the Gulf of
- transport of toxic Alexandrium fundyense populations within a coastal plume in the Gulf of Maine. Deep. Res. Part II Top. Stud. Oceanogr. 52, 2674–2697.

 https://doi.org/10.1016/j.dsr2.2005.06.016

 Large, W.G., Pond, S., 1981. Open Ocean Momentum Flux Measurements in Moderate to Strong Winds. J. Phys. Oceanogr. https://doi.org/10.1175/1520-
- Lema, K.A., Latimier, M., Nézan, É., Fauchot, J., Le Gac, M., 2017. Inter and intra-specific growth and domoic acid production in relation to nutrient ratios and concentrations in Pseudonitzschia: phosphate an important factor. Harmful Algae 64, 11–19.
- 734 https://doi.org/10.1016/j.hal.2017.03.001

0485(1981)011<0324:OOMFMI>2.0.CO;2

- Li, Y., He, R., 2014. Spatial and temporal variability of SST and ocean color in the Gulf of Maine based on cloud-free SST and chlorophyll reconstructions in 2003-2012. Remote Sens.
- 737 Environ. 144, 98–108. https://doi.org/10.1016/j.rse.2014.01.019

- 738 Li, Y., He, R., McGillicuddy, D.J., 2014. Seasonal and interannual variability in Gulf of Maine
- hydrodynamics: 2002-2011. Deep. Res. Part II Top. Stud. Oceanogr. 103, 210–222.
- 740 https://doi.org/10.1016/j.dsr2.2013.03.001
- 741 Li, Y., He, R., McGillicuddy, D.J., Anderson, D.M., Keafer, B.A., 2009. Investigation of the 2006
- Alexandrium fundyense bloom in the Gulf of Maine: In-situ observations and numerical
- 743 modeling. Cont. Shelf Res. 29, 2069–2082. https://doi.org/10.1016/j.csr.2009.07.012
- Lundholm, N., Clarke, A., Ellegaard, M., 2010. A 100-year record of changing Pseudo-nitzschia
- species in a sill-fjord in Denmark related to nitrogen loading and temperature. Harmful
- 746 Algae 9, 449–457. https://doi.org/10.1016/j.hal.2010.03.001
- Lundholm, N., Krock, B., John, U., Skov, J., Cheng, J., Panči, M., Wohlrab, S., Rigby, K., Nielsen,
- 748 T.G., Selander, E., Harðardóttir, S., 2018. Induction of domoic acid production in diatoms—
- 749 Types of grazers and diatoms are important. Harmful Algae.
- 750 https://doi.org/10.1016/j.hal.2018.06.005
- The Lynch, D.R., Naimie, C.E., 1993. Tide and its residual on the outer banks of the Gulf of Maine. J.
- 752 Phys. Oceanogr. https://doi.org/10.1175/1520-0485(1993)023<2222:TMTAIR>2.0.CO;2
- 753 MacFadyen, A., Hickey, B.M., Foreman, M.G.G., 2005. Transport of surface waters from the
- Juan de Fuca eddy region to the Washington coast. Cont. Shelf Res. 25, 2008–2021.
- 755 https://doi.org/10.1016/j.csr.2005.07.005
- 756 Marchetti, A., Trainer, V.L., Harrison, P.J., 2004. Environmental conditions and phytoplankton
- dynamics associated with Pseudo-nitzschia abundance and domoic acid in the Juan de
- 758 Fuca eddy. Mar. Ecol. Prog. Ser. 281, 1–12. https://doi.org/10.3354/meps281001
- 759 Martin-Jézéquel, V., Calu, G., Candela, L., Amzil, Z., Jauffrais, T., Séchet, V., Weigel, P., 2015.
- 760 Effects of organic and inorganic nitrogen on the growth and production of domoic acid by
- 761 Pseudo-nitzschia multiseries and P. australis (bacillariophyceae) in culture. Mar. Drugs 13,
- 762 7067–7086. https://doi.org/10.3390/md13127055
- 763 McCabe, R.M., Hickey, B.M., Kudela, R.M., Lefebvre, K.A., Adams, N.G., Bill, B.D., Gulland,
- 764 F.M.D., Thomson, R.E., Cochlan, W.P., Trainer, V.L., 2016. An unprecedented coastwide
- toxic algal bloom linked to anomalous ocean conditions. Geophys. Res. Lett. 43, 10,366-
- 766 10,376. https://doi.org/10.1002/2016GL070023

- McGillicuddy, D.J., Townsend, D.W., He, R., Keafer, B. a, Kleindinst, J.L., Li, Y., Manning, J.P.,
- Mountain, D.G., Thomas, M. a, Anderson, D.M., 2011. Suppression of the 2010
- Alexandrium fundyense bloom by changes in physical, biological, and chemical properties
- of the Gulf of Maine. Limnol. Oceanogr. 56, 2411–2426.
- 771 https://doi.org/10.4319/lo.2011.56.6.2411
- 772 Morrison, J.R., 2019. No Title [WWW Document]. Northeast. Reg. Assoc. Coast. Ocean Obs.
- 773 Syst. URL http://neracoos.org/
- Palma, S., Mouriño, H., Silva, A., Barão, M.I., Moita, M.T., 2010. Can Pseudo-nitzschia blooms be
- modeled by coastal upwelling in Lisbon Bay? Harmful Algae 9, 294–303.
- 776 https://doi.org/10.1016/j.hal.2009.11.006
- Parsons, M.L., Dortch, Q., Turner, R.E., 2002. Sedimentological evidence of an increase in
- Pseudo-nitzschia (Bacillariophyceae) abundance in response to coastal eutrophication.
- 779 Limnol. Oceanogr. 47, 551–558. https://doi.org/10.4319/lo.2002.47.2.0551
- 780 Pettigrew, N.R., Churchill, J.H., Janzen, C.D., Mangum, L.J., Signell, R.P., Thomas, A.C.,
- Townsend, D.W., Wallinga, J.P., Xue, H., 2005. The kinematic and hydrographic structure of
- the Gulf of Maine Coastal Current. Deep. Res. Part II Top. Stud. Oceanogr. 52, 2369–2391.
- 783 https://doi.org/10.1016/j.dsr2.2005.06.033
- Quijano-Scheggia, S., Garcés, E., Flo, E., Fernández-Tejedor, M., Diogène, J., Camp, J., 2008.
- 785 Bloom dynamics of the genus Pseudo-nitzschia (Bacillariophyceae) in two coastal bays (NW
- 786 Mediterranean Sea). Sci. Mar. 72, 577–590. https://doi.org/10.3989/scimar.2008.72n3577
- 787 Rappaport, S., 2016. Shellfish closure expanded; cost to industry mounts. Ellsworth Am.
- Ryan, J.P., Kudela, R.M., Birch, J.M., Blum, M., Bowers, H.A., Chavez, F.P., Doucette, G.J.,
- Hayashi, K., Marin, R., Mikulski, C.M., Pennington, J.T., Scholin, C.A., Smith, G.J., Woods, A.,
- 790 Zhang, Y., 2017. Causality of an extreme harmful algal bloom in Monterey Bay, California,
- 791 during the 2014–2016 northeast Pacific warm anomaly. Geophys. Res. Lett. 44, 5571–
- 792 5579. https://doi.org/10.1002/2017GL072637
- 793 Santiago-Morales, I.S., García-Mendoza, E., 2011. Growth and domoic acid content of Pseudo-
- 794 nitzschia australis isolated from northwestern Baja California, Mexico, cultured under
- 5795 batch conditions at different temperatures and two Si:NO3 ratios. Harmful Algae 12, 82–

796 94. https://doi.org/10.1016/j.hal.2011.09.004 797 Schnetzer, A., Jones, B.H., Schaffner, R.A., Cetinic, I., Fitzpatrick, E., Miller, P.E., Seubert, E.L., 798 Caron, D.A., 2013. Coastal upwelling linked to toxic Pseudo-nitzschia australis blooms in 799 Los Angeles coastal waters, 2005-2007. J. Plankton Res. 35, 1080–1092. 800 https://doi.org/10.1093/plankt/fbt051 801 Schwing, F.B., O'Farrel, M., Steger, J.M., Baltz, K., 1996. Coastal upwelling indices, West Coast of 802 North America, 1946-1995. NOAA Tech. Memo. NMFS-SWFSC-231 671, 1-45. 803 Sekula-Wood, E., Benitez-Nelson, C., Morton, S., Anderson, C., Burrell, C., Thunell, R., 2011. 804 Pseudo-nitzschia and domoic acid fluxes in Santa Barbara Basin (CA) from 1993 to 2008. 805 Harmful Algae 10, 567–575. https://doi.org/10.1016/J.HAL.2011.04.009 806 Smith, J., Connell, P., Evans, R.H., Gellene, A.G., Howard, M.D.A., Jones, B.H., Kaveggia, S., 807 Palmer, L., Schnetzer, A., Seegers, B.N., Seubert, E.L., Tatters, A.O., Caron, D.A., 2018. A 808 decade and a half of Pseudo-nitzschia spp. and domoic acid along the coast of southern 809 California. Harmful Algae 79, 87–104. https://doi.org/10.1016/j.hal.2018.07.007 810 Smith, J., Gellene, A.G., Hubbard, K.A., Bowers, H.A., Kudela, R.M., Hayashi, K., Caron, D.A., 811 2017. Pseudo-nitzschia species composition varies concurrently with domoic acid 812 concentrations during two different bloom events in the Southern California Bight. J. 813 Plankton Res. 40, 1–17. https://doi.org/10.1093/plankt/fbx069 814 Tammilehto, A., Nielsen, T.G., Krock, B., Møller, E.F., Lundholm, N., 2015. Induction of domoic 815 acid production in the toxic diatom Pseudo-nitzschia seriata by calanoid copepods. Aguat. 816 Toxicol. 159, 52-61. https://doi.org/10.1016/j.aquatox.2014.11.026 817 Tatters, A.O., Fu, F.X., Hutchins, D.A., 2012. High CO 2 and silicate limitation synergistically 818 increase the toxicity of Pseudo-nitzschia fraudulenta. PLoS One 7. 819 https://doi.org/10.1371/journal.pone.0032116 820 Terseleer, N., Gypens, N., Lancelot, C., 2013. Factors controlling the production of domoic acid 821 by Pseudo-nitzschia (Bacillariophyceae): A model study. Harmful Algae 24, 45–53. 822 https://doi.org/10.1016/j.hal.2013.01.004 823 Thessen, A.E., Stoecker, D.K., 2008. Distribution, abundance and domoic acid analysis of the 824 toxic diatom genus Pseudo-nitzschia from the Chesapeake Bay. Estuaries and Coasts 31,

825 664–672. https://doi.org/10.1007/s12237-008-9053-8 826 Thorel, M., Claquin, P., Schapira, M., Le Gendre, R., Riou, P., Goux, D., Le Roy, B., Raimbault, V., 827 Deton-Cabanillas, A.F., Bazin, P., Kientz-Bouchart, V., Fauchot, J., 2017. Nutrient ratios 828 influence variability in Pseudo-nitzschia species diversity and particulate domoic acid 829 production in the Bay of Seine (France). Harmful Algae 68, 192–205. 830 https://doi.org/10.1016/j.hal.2017.07.005 831 Townsend, D.W., McGillicuddy, D.J., Thomas, M.A., Rebuck, N.D., 2014. Nutrients and water 832 masses in the Gulf of Maine-Georges Bank region: Variability and importance to blooms of 833 the toxic dinoflagellate Alexandrium fundyense. Deep. Res. Part II Top. Stud. Oceanogr. 834 103, 238–263. https://doi.org/10.1016/j.dsr2.2013.08.003 835 Townsend, D.W., Pettigrew, N.R., Thomas, M.A., Neary, M.G., Mcgillicuddy, D.J., Donnell, J.O., 836 2015. Water masses and nutrient sources to the Gulf of Maine. J. Mar. Res. 141, 93–122. 837 https://doi.org/10.1038/141548c0 838 Townsend, D.W., Rebuck, N.D., Thomas, M.A., Karp-Boss, L., Gettings, R.M., 2010. A changing 839 nutrient regime in the Gulf of Maine. Cont. Shelf Res. 30, 820-832. 840 https://doi.org/10.1016/j.csr.2010.01.019 841 Townsend, D.W., Thomas, A.C., Mayer, L.M., Thomas, M.A., Quinlan, J.A., 2006. Oceanography 842 of the Northwest Atlantic Shelf (1, W), in: The Sea: The Global Coastal Ocean: 843 Interdisciplinary Regional Studies and Syntheses. Harvard University Press, pp. 119–168. 844 Trainer, V.L., Bates, S.S., Lundholm, N., Thessen, A.E., Cochlan, W.P., Adams, N.G., Trick, C.G., 845 2012. Pseudo-nitzschia physiological ecology, phylogeny, toxicity, monitoring and impacts 846 on ecosystem health. Harmful Algae 14, 271-300. 847 https://doi.org/10.1016/j.hal.2011.10.025 848 Trainer, V.L., Hickey, B.M., Horner, R.A., 2002. Biological and physical dynamics of domoic acid 849 production off the Washington coast. Limnol. Oceanogr. 47, 1438–1446. 850 https://doi.org/10.4319/lo.2002.47.5.1438 851 Trainer, V.L., Hickey, B.M., Lessard, E.J., Cochlan, W.P., Trick, C.G., Wells, M.L., MacFadyen, A., 852 Moore, S.K., 2009. Variability of Pseudo-nitzschia and domoic acid in the Juan de Fuca 853 eddy region and its adjacent shelves. Limnol. Oceanogr. 54, 289–308.

854	https://doi.org/10.4319/lo.2009.54.1.0289
855	Twardowski, M.S., Townsend, D.W., Sullivan, J.M., Koch, C., Pettigrew, N.R., O'Donnell, J.,
856	Stymiest, C., Salisbury, J., Moore, T., Young-Morse, R., Stockley, N.D., Morrison, J.R., 2015.
857	Developing the first operational nutrient observatory for ecosystem, climate, and hazard
858	monitoring for NERACOOS. Mar. Technol. Soc. J. 49, 72–80.
859	https://doi.org/10.4031/MTSJ.49.3.11
860	USGS, 2013. Water Data for the Nation [WWW Document]. URL
861	https://waterdata.usgs.gov/nwis
862	Wang, Z., King, K.L., Ramsdell, J.S., Doucette, G.J., 2007. Determination of domoic acid in
863	seawater and phytoplankton by liquid chromatography-tandem mass spectrometry. J.
864	Chromatogr. A 1163, 169–176. https://doi.org/10.1016/j.chroma.2007.06.054
865	Wells, M.L., Trick, C.G., Cochlan, W.P., Hughes, M.P., Trainer, V.L., 2005. Wells, Mark L., Charles
866	G. Trick, William P. Cochlan, Margaret P. Hughes, and Vera L. Trainer. Domoic acid: The
867	synergy of iron, copper, and the toxicity of diatoms. Limnol. Oceanogr., 50(6), 2005, 1908–
868	1917. Limnol. Ocean. 50, 1908–1917.
869	Xue, H., Chai, F., Pettigrew, N.R., 2000. A Model Study of the Seasonal Circulation in the Gulf of
870	Maine. J. Phys. Oceanogr. 30, 1111–1135. https://doi.org/10.1175/1520-
871	0485(2000)030<1111:AMSOTS>2.0.CO;2
872	
873	

8 Tables

Table 1 - Summary of physical and biological time series and survey data. MDIBL = Mt. Desert Island Biological Laboratory; NO_{x}^{-} = nitrate + nitrite; NH_{4}^{+} = ammonium; $Si(OH)_{4}$ = silicic acid; PO_{4}^{3-} = phosphate

Sample Dates	Parameters
Aug 2012, Jul 2014,	Temperature, Salinity,
Aug 2015, Oct 2016	NO _x -, NH ₄ +, Si(OH) ₄ , PO ₄ ³⁻ ,
	Pseudo-nitzschia cell counts,
	Species Relative Abundance
Jul-Nov 2013, Jun-Oct 2014,	All years: <i>Pseudo-nitzschia</i> cell counts
Feb-Sep 2015, Jun-Oct 2016	2013 only: Temperature, Salinity,
	NO _x -, NH ₄ +, Si(OH) ₄ , PO ₄ ³⁻ ,
	Species Relative Abundance
Continuous 2002-2017	Temperature, Salinity,
	Air temperature, Air Pressure, Wind Speed
Varied	Daily discharge
	Aug 2012, Jul 2014, Aug 2015, Oct 2016 Jul-Nov 2013, Jun-Oct 2014, Feb-Sep 2015, Jun-Oct 2016 Continuous 2002-2017

Table 2 - Presence/Absence of Pseudo-nitzschia species 2012-2016. An 'X' indicates that in at least one sample the ARISA measured >0 relative abundance for that species in that year.

	P. delicatissima	P. plurisecta	P. pungens	P. seriata	P. australis	P. caciantha	P. cuspidata	P. fraudulenta	P. heimii/americana	P. obtusa
2012	Х	Х	Χ	Χ			Х		Х	Х
2013	Х	Χ	Χ	Χ			Χ	X	Χ	Χ
2014	Х	Χ	Χ	Χ		Χ	Χ			
2015	Χ	Χ	X	Χ		Χ	Х	Х	Χ	
2016	Χ	Χ	X	Χ	Χ			Χ	Χ	

Year(s)	Species	R ²
2012	P. plurisecta	0.33
2012	Total cell count	0.47
2013	P. plurisecta	0.53
2014	P. plurisecta	0.29
2014	Total cell count	0.17
2016	P. australis	0.22
2016	Total cell count	0.66
2012-2016	P. australis	0.19
2012-2016	Total cell count	0.53

9 Figure Captions

- 1. Figure 1: (A) Climatological circulation of the GOM as described in Pettigrew et al., (2005) and adapted in Anderson et al., (2005) (Used with permission). (B) Locations of hydrographic instruments and the 2016 *Pseudo-nitzschia* ship survey in the GOM. "Mt Desert Island" is shown, where both MDIBL and Bar Harbor are located.
 - 2. Figure 2: From the MDIBL and Bar Harbor time series data, *Pseudo-nitzschia* spp. cell concentration versus time in 2013, 2014, 2015, and 2016. Timing of the 2014, 2015, and 2016 cruises are indicated with vertical lines. Maximum total cell abundance from each cruise is plotted as a single point. Note that the y axis scales are different.
 - 3. Figure 3: From the Bar Harbor time series, *Pseudo-nitzschia* cell concentration (left axis; blue line) and pDA (right axis; red Xs) versus time in 2013. Relative species abundance for each sample is indicated with pie charts.
 - 4. Figure 4: (Left) August 2012 species relative abundance of surface samples plotted on the sampling locations in the GOM. Pie chart size was determined by log(cell count) (scale shown at lower right). (Right) 2012 relative species abundance on a salinity vs. cell count diagram, with axes scaled to match Figure 5, Figure 6, and Figure 7.
 - 5. Figure 5: (Left) July 2014 species relative abundance of surface samples plotted on the sampling locations in the GOM. Pie chart size was determined by log(cell count) (scale shown at lower right). (Right) 2014 relative species abundance on a salinity vs. cell count diagram, with axes scaled to match Figure 4, Figure 6, and Figure 7.
 - 6. Figure 6: (Left) August 2015 species relative abundance of surface samples plotted on the sampling locations in the GOM. Pie chart size was determined by log(cell count) (scale shown at lower right). (Right) 2015 relative species abundance on a salinity vs. cell count diagram, with axes scaled to match Figure 4, Figure 5, and Figure 7.
 - 7. Figure 7: (Left) October 2016 species relative abundance of surface samples plotted on the sampling locations in the GOM. Pie chart size was determined by log(cell count) (scale shown at lower right). (Right) 2016 relative species abundance on a salinity vs. cell count diagram, with axes scaled to match Figure 4, Figure 5, and Figure 6.

915 8. Figure 8: Box-and-Whisker plots of particulate DA measured during August 2012, June–
916 October 2013, July 2014, August 2015, and October 2016. Note that the y axis is a log
917 scale. The crosses are outliers, defined as points greater than (less than) Q3(Q1) +(-)
918 1.5*(Q3-Q1), where Q1 is the first quartile and Q3 is the third quartile.

- 9. Figure 9: Relative species abundance for each survey cruise on a particulate DA vs log(cell count) diagram: (A) 2012, (B) 2014, (C) 2015, (D) 2016. Note that the axes scales are not constant.
- 10. Figure 10: (A) Cumulative Upwelling Index vs time in 2012–2016, calculated with atmospheric data from NERACOOS Station I. (B) Temperature and salinity measurements from all ship surveys plotted on one temperature-salinity diagram. Climatological means (circles) and minima/maxima (error bars) of temperature and salinity for the months July, August, and October (the same months as the cruise surveys) are also shown from NERACOOS station I.
- 11. Figure 11: Salinity (top) and temperature (bottom) climatology as measured by NERACOOS buoy station M (Jordan Basin) at 250m. Climatology was calculated from data measured in 2003–2019, and 2016 daily means are overlain.